



Preparation of Hierarchically Porous Carbon Materials from  
Sugarcane Bagasse

Ratchadaporn Kueasook

A Thesis Submitted in Partial Fulfillment of the Requirements for the  
Degree of Master of Science in Chemistry (Physical Chemistry)

Prince of Songkla University

2018

Copyright of Prince of Songkla University



Preparation of Hierarchically Porous Carbon Materials from  
Sugarcane Bagasse

Ratchadaporn Kueasook

A Thesis Submitted in Partial Fulfillment of the Requirements for the  
Degree of Master of Science in Chemistry (Physical Chemistry)

Prince of Songkla University

2018

Copyright of Prince of Songkla University

**Thesis Title** Preparation of Hierarchically Porous Carbon Materials from Sugarcane Bagasse

**Author** Miss Ratchadaporn Kueasook

**Major Program** Chemistry (Physical Chemistry)

---

**Major Advisor**

.....  
(Dr. Laemthong Chuenchom)

**Examining Committee :**

.....Chairperson  
(Dr. Decha Dechtrirat)

.....Committee  
(Assoc. Prof. Dr. Pongsaton Amornpitoksuk)

.....Committee  
(Asst. Prof. Dr. Uraivan Sirimahachai)

.....Committee  
(Dr. Laemthong Chuenchom)

The Graduate School, Prince of Songkla University, has approved this thesis as partial fulfillment of the requirements for the Master of Science Degree in Chemistry (Physical Chemistry).

.....  
(Prof. Dr. Damrongsak Faroongsarng)  
Dean of Graduate School

This is to certify that the work here submitted is the result of the candidate's own investigations. Due acknowledgement has been made of any assistance received.

.....Signature

(Dr. Laemthong Chuenchom)

Major Advisor

.....Signature

(Miss Ratchadaporn Kueasook)

Candidate

I hereby certify that this work has not been accepted in substance for any degree, and is not being currently submitted in candidature for any degree.

.....Signature

(Miss Ratchadaporn Kueasook)

Candidate

ชื่อวิทยานิพนธ์ การเตรียมวัสดุคาร์บอนที่มีรูพรุนขนาดกลางและขนาดใหญ่จากชานอ้อย

ผู้เขียน นางสาวรัชฎาพร เกื้อสุข

สาขาวิชา เคมี (เคมีเชิงฟิสิกส์)

ปีการศึกษา 2561

### บทคัดย่อ

วัสดุคาร์บอนที่มีรูพรุนแบบลำดับชั้น (Hierarchically porous carbon materials : HPC) ถูกเตรียมขึ้นด้วยวิธี Soft-templating self-assembly โดยใช้ Phloroglucinol/ Glyoxylic acid เป็นแหล่งให้คาร์บอนและใช้ Pluronic triblock copolymer F127 เป็นแม่แบบรูพรุนขนาดกลาง (ขนาดรูพรุน 2-50 นาโนเมตร) บนผิวของชานอ้อย โดยได้ศึกษาผลของอัตราส่วนระหว่าง แหล่งให้คาร์บอน (carbon precursor) ต่อแม่แบบรูพรุนขนาดกลาง (template) ที่มีผลต่อลักษณะของรูพรุน อีกทั้งยังมีการเตรียมวัสดุคาร์บอนที่ไม่มีแม่แบบรูพรุนขนาดกลาง (BG\_PGF) และวัสดุคาร์บอนที่เกิดจากการเผาชานอ้อยเพียงอย่างเดียว (BG) โดยไม่มีแม่แบบ และยังได้ศึกษาลักษณะทางกายภาพและทางเคมีของวัสดุที่เตรียมได้ด้วยเทคนิคหลายประเภท พบว่าวัสดุที่เตรียมได้ทั้งหมดมีลักษณะทางเคมีที่คล้ายคลึงกันมาก แต่มีลักษณะรูพรุนที่แตกต่างกัน คือ BG และ BG\_PGF มีรูพรุนขนาดเล็กเพียงชนิดเดียว (ขนาดรูพรุน < 2nm) ส่วน HPC มีรูพรุนขนาดกลาง (ขนาดของรูพรุนอยู่ระหว่าง 5-6 nm) เมื่อเปรียบเทียบความสามารถในการดูดซับเมธิลีนบลู ปรากฏว่า ค่าการดูดซับสูงสุดของ HPC สูงกว่า BG\_PGF และ BG แสดงให้เห็นว่ารูพรุนขนาดกลางเป็นปัจจัยสำคัญในการดูดซับ ดังนั้นวิธีการเตรียมวัสดุคาร์บอนที่มีรูพรุนแบบลำดับชั้น (HPC) ในงานวิจัยนี้ เป็นวิธีที่สามารถเตรียมได้ง่าย ใช้สารที่ไม่ก่อให้เกิดมลพิษ อีกทั้งวัสดุคาร์บอนที่เตรียมได้นี้มีลักษณะเป็นชิ้นงาน เมื่อนำไปใช้เป็นตัวดูดซับ สามารถแยกออกจากระบบได้ง่าย

<b>Thesis Title</b>	Preparation of Hierarchically Porous Carbon Materials from Sugarcane Bagasse.
<b>Author</b>	Miss Ratchadaporn Kueasook
<b>Major program</b>	Chemistry (Physical Chemistry)
<b>Academic Year</b>	2018

### ABSTRACT

Hierarchically porous carbon materials (HPC) were successfully prepared from environmentally friendly phloroglucinol/glyoxylic acid precursors with soft-template F127 using sugarcane bagasse as scaffold by self-assembly method. Phloroglucinol and glyoxylic acid used as carbon precursor and F127 as a mesopore template. Effect of carbon precursor/template ratio on the physical and chemical properties of the carbon monoliths was studied. The sample without template (BG\_PGF) was prepared by carbonizing the sugarcane bagasse mixed with carbon precursor under the same conditions. Furthermore, various techniques were employed to investigate the physicochemical properties of the carbon monoliths. While the chemical properties of monolith adsorbents are the same, the physical properties are different. BG\_PGF and BG have only micropore (pore size <2 nm). HPC has mesopore (pore size 2-50 nm). Moreover, The maximum adsorption capacity of methylene blue for HPC higher than BG\_PGF and BG. It showed the mesopore structure are the factor for adsorption property. The coated carbon was highly stable mechanical stability than BG. The obtained HPC has a great potential as a floating monolith adsorbent for water treatment.

## ACKNOWLEDGEMENTS

I would like to express my sincere thanks to my advisor, Dr. Laemthong Cheunchom, who has suggested this research problem, for his numerous comments, encouragement, criticism and kindness during the laboratory work and the preparation of this thesis.

I am grateful to Assoc. Prof. Dr. Pongsaton Amornpitoksuk and Asst. Prof. Dr. Uraivan Sirimahachai, who have given their times in reviewing the text and suggested the improvement of the report. I am also grateful to Dr. Decha Dechtrirat, the examining chairperson for his kind comments and correction of this thesis.

I would like to thank the staff of the Department of Chemistry and also many other people, friends who are involved, especially the members of Ch314 for their help and encouragement during my study.

I am grateful to the Department of Chemistry, Faculty of Science, Prince of Songkla University, Hat Yai; Research Assistantship (RA, Contract No. 1-2558-02-002) of the Faculty of Science and the Graduate School, Prince of Songkla University for their financial supports.

Love, encouragement from my family and friends will be remembered.

Ratchadaporn Kueasook



## THE RELEVANCE OF THE RESEARCH WORK TO THAILAND

Sugarcane bagasse is the most agricultural waste of sugar industry, and is abundantly available, mainly in Thailand. Sugarcane bagasse has been employed for other applications such as manufacturing pulp and paper, furniture, electricity, there are few reports on the application of sugarcane bagasse.

Therefore, the aim of this thesis was to prepare the hierarchically porous carbon materials (HPC) from environmentally friendly phloroglucinol/glyoxylic acid precursors with soft-templated F127 using sugarcane bagasse as scaffold, and to study the adsorption of methylene blue. To provide an understanding the experimental results using information from various characterization techniques.

## CONTENTS

	Page
บทคัดย่อ .....	v
ABSTRACT .....	vi
ACKNOWLEDGEMENTS .....	vii
THE RELEVANCE OF THE RESEARCH WORK TO THAILAND.....	viii
CONTENTS .....	ix
LIST OF FIGURES.....	xi
LIST OF TABLES .....	xiii
INTRODUCTION .....	1
1.1 Introduction.....	1
1.2 Preliminary knowledge and Theoretical section .....	3
1.2.1 Definition of hierarchical porous carbon .....	3
1.2.2 Type of hierarchical porous material preparation.....	4
1.2.3 Principles of soft-templating of mesoporous carbon using amphiphilic block-copolymers.....	5
1.2.4 Adsorption.....	5
1.3 Review of literature .....	8
1.4 Objectives .....	10
EXPERIMENTAL .....	12
2.1 Chemicals and materials .....	12
2.2 Equipment and instruments.....	12
2.3 Methods.....	13

2.3.1 Preparation of monolithic hierarchical porous carbon materials.....	13
2.3.2 Characterization of monolithic hierarchical porous carbon materials .....	15
2.3.3 Adsorption studies.....	17
RESULTS AND DISCUSSION.....	19
3.1 Formation of hierarchical porous structures.....	19
3.2 Characterization of hierarchical porous structures .....	21
3.3 Adsorption of dye by hierarchical porous carbon materials .....	36
3.3.1 Adsorption kinetics of methylene blue by hierarchical porous carbon materials.....	36
3.3.2 Adsorption isotherm of methylene blue by hierarchical porous carbon materials.....	40
3.3.3 Adsorbent regeneration of hierarchically porous carbon monoliths.....	47
CONCLUSION.....	49
BIBLIOGRAPHY.....	50
VITAE.....	54

## LIST OF FIGURES

	Page
<b>Figure 1</b> Schematic Illustration of the preparation steps for all HPC by Self-Assembly Methods.....	15
<b>Figure 2</b> Photograph of the samples contained analysis tube without being ground.	16
<b>Figure 3</b> Optical images of (A) Sugarcane Bagasse(BG), (B) Composite HPC(2.4), (C) HPC(2.4)_800 and (D) HPC(2.4)_800A.....	19
<b>Figure 4</b> SEM and TEM analysis. (A) SEM image at 500x of sugarcane bagasse (sectional areas of the vessels), (B-C) SEM images at 500x-800x of HPC(2.4)_800A (sectional areas of the vessels), (D-E) FE-SEM image at 300000x-600000x of HPC(2.4)_800A and (F-G) TEM image at 500x of HPC(2.4)_800A.....	22
<b>Figure 5</b> Nitrogen adsorption-desorption isotherm of (A-D) samples before air oxidation, (E-H) samples after air oxidation.....	24
<b>Figure 6</b> Mesopore size distribution using BJH model of all samples. ....	25
<b>Figure 7</b> Micropore size calculated by DFT method of all samples. ....	26
<b>Figure 8</b> Functional group from FTIR spectrum of all samples.....	29
<b>Figure 9</b> Survey spectrum from XPS of all samples.....	32
<b>Figure 10</b> High-resolution XPS spectra of (A) C1s of HPC(2.4)_800, (B) C1S of HPC(2.4)_800A, (C) O1s of HPC(2.4)_800 and (D) O1s of HPC(2.4)_800A. ....	34
<b>Figure 11</b> Effect of contact time on the methylene blue adsorption over (A) All samples before air oxidation and (B) All samples after air oxidation. Reaction conditions: Initial concentration 40 ppm, temperature $30\pm 2^{\circ}\text{C}$ and adsorbent dosage 0.03 g/25 mL. ...	36
<b>Figure 12</b> Photographs of MB solution after adsorption by HPC(2.4)_800A and MB adsorption by BG_800A and BG_PGF_800A as a control. ....	37
<b>Figure 13</b> Adsorption isotherm of methylene blue onto all monolith (A) All samples before air oxidation and (B) All samples after air oxidation. Reaction conditions: initial concentration 40-850 mg/g, temperature $30\pm 2^{\circ}\text{C}$ and adsorbent dosage 0.03 g/25 mL. ....	40

<b>Figure 14</b> Adsorption isotherm for methylene blue (MB), methyl orange (MO) and Rhodamine B (RhB) on HPC(2.4)_800A. ....	42
<b>Figure 15</b> Correlation of adsorption affinity of different (A) surface area (B) micropore area (C) mesopore area and (D) mesopore volume.....	44
<b>Figure 16</b> Schematic Illustration of the effect of pore morphology on the adsorption performance of MB. ....	45
<b>Figure 17</b> The reusability of HPC(2.4)_800A.....	47

## LIST OF TABLES

	Page
<b>Table 1.</b> Table 1. Chemical structure, Molecular size, Molecular weight, $\lambda_{\max}$ of UV/Visible adsorption for dyes. ....	17
<b>Table 2</b> Detail texture properties measured by nitrogen sorption at 77K .....	27
<b>Table 3.</b> Assignment of peaks in FTIR of samples. ....	30
<b>Table 4</b> The percentage compositions from XPS of all samples .....	33
<b>Table 5</b> Assignment of peak from XPS (C 1s and O 1s) for HPC(2.4)_800 and HPC(2.4)_800A. ....	35
<b>Table 6</b> Fitted parameters in the pseudo second order model for methylene blue 40 mg/g onto samples before air oxidation. ....	39
<b>Table 7</b> Fitted parameters in the pseudo second order model for methylene blue 40 mg/g onto samples after air oxidation. ....	39
<b>Table 8</b> Fitted parameters values in Langmuir adsorption isotherm for methylene blue adsorption onto samples before air oxidation. ....	41
<b>Table 9</b> Fitted parameters values in Langmuir adsorption isotherm for methylene blue adsorption onto samples after air oxidation. ....	41
<b>Table 10</b> Literature review on monolith adsorbents for dye removal and results. ....	47

## CHAPTER 1

### INTRODUCTION

#### 1.1 Introduction

Waste water from oil, organic chemicals, dyes and heavy metals are generated by textile industry, paper industry, paint industry, tanning industry and metal industry. Dyes are considered to be the major pollutants in the industrial effluents because of their toxicity and carcinogenic (Vorosmarty, McIntyre et al. 2010). There are various types of dyes categorized by their electric charge and size. Namely, cationic dye, anionic dye, and bulky dye which methylene blue (MB), methyl orange (MO), and rhodamine B (RhB) were selected to be the representatives in this research, respectively (Gupta and Suhas 2009).

Therefore, the treatment of wastewater containing dyes is globally crucial. The treatment techniques for dye removal include coagulation and flocculation, oxidation, photocatalysis, biosorption and adsorption (Wan Ngah and Hanafiah 2008). Adsorption is considered one of the most efficient methods because of its simple, low cost and flexibility (Bhatnagar and Sillanpää 2010).

In recent years, carbon-based materials, including activated carbons (Bastami and Entezari 2012), carbon nanotubes (CNTs) (Stafiej and Pyrzynska 2007), graphene, graphene oxides (GOs), carbon aerogels and other carbon nanostructures have become an important class of materials of choice due to their unique chemical and physical properties (Chen, Ma et al. 2015). Their high thermal, physical, and chemical stabilities under strong conditions e.g., high temperature and under strong acid/basic conditions, make them ideal for long-lasting application performance in real water treatment. Besides, carbonaceous materials are in general environmentally friendly, inexpensive, and easy to be functionalized. Activated carbons (Malik 2004), CNTs (Stafiej and Pyrzynska 2007) and graphene, GOs have widely been employed for the water remediation.

However, the low cost activated carbons still have its own disadvantages in the preparation step such as the use of toxic chemicals, high temperature in carbonization and activation process, and complicated step.

Nevertheless, they are generally in the form of fine powder. These small particle sizes of activated carbons, CNTs and unassembled graphene make them difficult to be completely collected and recycled after usage, which may cause secondary environmental pollution. Moreover, these materials possess almost the microporous structure which is not suitable for the adsorption of dye molecule ( $M_w > 200$ ). On the contrary, carbon-based materials with a macroscopic bulky shape are easier to be manipulated and collected. To solve this problem, granular and monolithic forms of composite adsorbent are the good alternative approach. However, their weakness is the usage of chemicals as binder causing more complicated preparation and the decreasing adsorption performance of materials. Therefore, the promising solution is to use binder-free method.

Whereas large pores and voids generally exist in CNT-, carbon aerogel-, and graphene-based 3D materials, mesoporous carbon materials represent another large category of unique structures with pore sizes between 2 -50 nm which are appropriate with the size of bulky dye molecule. These mesopores are typically produced based on the self-assembly of carbon precursor molecules with the soft templates to form organic-organic composites, and mesoporous carbons are obtained after subsequent carbonization. Using micelles of amphiphilic block copolymers as soft templates, facile control over the morphology and size of mesopores can be achieved. However, the presence of such unimodal pore systems, including macropores ( $> 50$  nm), mesopores (2-50 nm), and micropores ( $< 2$  nm) alone limit their performance in various applications, including the water remediation. The hierarchical pore texture could then be a solution to problems. Such hierarchical structures are characterized by the presence of macropores together with micro- and/or mesopores. The presence of macropores is desirable because these bigger pores can act as a transport system for liquids and gases, thus enhancing the accessibility of the smaller pores. Therefore,



monolithic carbon materials with a hierarchical macro- and mesoporous character would be a good choice for the adsorption of dyes (Zhuang, Wan et al. 2009).

There were previously reports using monolithic-formed adsorbent. All of them employed the formaldehyde as carbon source and cross-linker which is terribly toxic and did not employ the concept of green chemistry (Wang, Xue et al. 2011, Xia, Li et al. 2015). Recently, Ghimbeu used glyoxylic acid and phloroglucinol as carbon precursor, and the evaporation was carried out at room temperature with simple step. (Matei Ghimbeu, Vidal et al. 2014). Therefore, the phloroglucinol/ glyoxylic acid polymer was coated with soft-templated method on natural scaffold sugarcane bagasse due to its natural macropore and scalable (Huang and Doong 2012).

In this research, hierarchically porous carbon materials (HPC) were prepared as monolithic form from environmentally friendly phloroglucinol/glyoxylic acid precursors with soft-templated F127 using sugarcane bagasse as scaffold. Finally, these novel HPCs were employed as adsorbents to investigate the potential performance in dye adsorption.

## **1.2 Preliminary knowledge and Theoretical section**

### **1.2.1 Definition of hierarchical porous carbon**

The hierarchically porous carbon materials (HPCs) possess pores of well-defined and interconnected porous structures both in the mesopore (pore size 2-50 nm) and macropore (pore size > 50 nm) regions. Macropores can provide highly efficient mass transport while mesopores can give rise to high surface area and large pore volumes, as well as act as active adsorption sites. The main motivation behind this activity is a combination of different pore sizes in the meso/macropore regions. (Sun, Chen et al. 2016)

### 1.2.2 Type of hierarchical porous material preparation

Hierarchically porous materials were synthesized in several ways :

(1) Post-treatment is stimulated by a chemical or thermal activation. (Yuan, Blin et al. 2002)

(2) Self-formation phenomenon. This method produces macro-, meso- and micropores occur at the walls of macropore by Hydrolysis/Condensation reaction of alkaloids in solution. This method was rapid but many factors must be controlled such as the central atom of the metal, the pH, and the temperature of the solution. (Deng and Shanks 2005, Li, Yang et al. 2010)

(3) Replication. This method based on three steps: preparing inorganic templates, burning and removing templates. Step of removing template, acid/base solution is required. So. This process was multi-step synthesis. This is a major drawback of this process. (Yoon, Sohn et al. 2002)

(4) Templating method (4.1) Hard-templating : The dual-templating strategy involve combination of two different porosities. Most of the templates is inorganic materials which involve multi-step, time consuming, high toxic chemical and not suitable for industry. (Machoke, Beltrán et al. 2015) (4.2) Self-templating : Self-template can provide an alternative facile way to control its mesopore structure. The dual-templating strategy are combined two different porosities. (Martins, Alves Rosa et al. 2010). (4.3) Multiple templating such as using a colloidal crystal as a template combined with soft-template. , using a polymers coat onto the natural macropore materials. (Hosseini, Khan et al. 2011, Zhang, Liu et al. 2011, Huang and Doong 2012, Elaigwu and Greenway 2014, Chen, Li et al. 2015, Xia, Li et al. 2015)

### 1.2.3 Principles of soft-templating of mesoporous carbon using amphiphilic block-copolymers.

Mesoporous carbon materials were synthesis by using micelles of amphiphilic block copolymers as a template such as poly(ethylene oxide)-b-poly(propylene oxide)-b-poly(ethylene oxide) triblock copolymers(PEO-b-PPO-b-PEO) from the Pluronic family, polystyrene-b-poly(4-vinylpyridine)(PSb-P4VP) or polystyrene-b-poly(ethylene oxide) (PS-b-PEO). The common carbon precursors are phenol/formaldehyde (or resol), recorcinol/ formaldehyde (or RF resin) and phloroglucinol/formaldehyde (or PF resin). The carbon precursor and template was mixed in solution. This mixture assembles into an ordered mesophase. The mesophase is stabilized via thermal or catalytic crosslinking. Finally, the template was removed and mesopores were generated during carbonization process. (Chuenchom, Kraehnert et al. 2012)

### 1.2.4 Adsorption

Adsorption is the attraction forces between adsorbate and adsorbent can come from Vander waal forces which are weak forces or from chemical bond which are strong one. On the basis of type of attraction forces between adsorbate and adsorbent, the adsorption process can be classified in two types: physical adsorption or chemical adsorption. Removal of the molecule from the surface is called desorption. (Helfferich, 1985; Marsh & Rodríguez-Reinoso, 2006b; Marsh & Rodríguez-Reinoso, 2006c).

#### (1) Physisorption

Where the adsobates were held by physical (i.e., Van der Waals) forces with the formation of multilayer of adsorbate on adsorbent. These forces can be eliminated (removal of molecules from surface of adsorbent) when increasing temperature. Therefore, physisorption can be called reversible process, and it also has low enthalpy of adsorption.

## (2) Chemisorption

Where there is direct chemical bond between the adsorbate and the surface of adsorbent with the formation of monolayer of adsorbate on adsorbent. This bond cannot be broken by only increased temperature. Therefore, this behavior is usually irreversible process, and it also has high enthalpy of adsorption.

### 1.2.3.1 Adsorption kinetics

#### (1) Pseudo first order

Lagergren (1898) presented a pseudo first-order rate equation to describe the kinetic process of liquid-solid phase adsorption of oxalic acid and malonic acid onto charcoal, which is believed to be the earliest model for determining the adsorption rate based on the adsorption capacity. It can be presented as follows:

$$\frac{dq_t}{t} = k_1(q_e - q_t) \quad (1)$$

Where  $q_e$  and  $q_t$  (mg/g) are the adsorption capacities at equilibrium and time  $t$  (min), respectively.  $k_1$  ( $\text{min}^{-1}$ ) is the pseudo-first-order rate constant. Integrating Eq. (1) with the boundary conditions of  $q_t = 0$  at  $t = 0$  and  $q_t = q_t$  at  $t = t$ , yields

$$\ln\left(\frac{q_e}{q_e - q_t}\right) = k_1 t \quad (2)$$

#### (2) Pseudo second order

In 1995, Ho described a kinetic process of the adsorption of divalent metal ions onto peat, in which the chemical bonding among divalent metal ions and polar functional groups on peat, such as aldehydes, ketones, acids, and phenolics are responsible for the cation-exchange capacity of the peat. It can be presented as follows:

$$\frac{dq_t}{t} = k_2(q_e - q_t)^2 \quad (3)$$

Integrating Eq. (3) with the boundary conditions of  $q_t = 0$  at  $t = 0$  and  $q_t = q_t$  at  $t = t$ , yields

$$\frac{t}{q_t} = \frac{t}{q_e} + \frac{1}{k_2 q_e^2} \quad (4)$$

### 1.2.3.2 Adsorption isotherm

#### (1) Langmuir isotherm

In 1916, Irving Langmuir published a new model isotherm for gases adsorbed to solids known as Langmuir Adsorption isotherm. It is a semi-empirical isotherm derived from a proposed kinetic mechanism. This isotherm was based on different assumptions one of which is that dynamic equilibrium exists between adsorbed gaseous molecules and the free gaseous molecules (Helfferich, 1985).

In the case of solution (solid-liquid adsorption), the non-linear Langmuir adsorption isotherm is expressed in Eq. (5)

$$q_e = \frac{q_m b C_e}{1 + b C_e} \quad (5)$$

Where  $q_e$  and  $q_m$  are equilibrium and maximum adsorption capacity (mg/g), respectively.  $b$  is the Langmuir isotherm coefficient and  $C_e$  is the equilibrium concentration of adsorbate.

However, many researchers have usually used linear form of Langmuir adsorption isotherm which easier to calculate and fit the data. The linear form is expressed in Eq. (6).

$$\frac{C_e}{q_e} = \frac{1}{b q_m} + \frac{C_e}{q_m} \quad (6)$$

#### (2) Freundlich isotherm

In 1909, Herbert Freundlich gave an empirical expression representing the relationship between the concentrations of a solute on the surface of an adsorbent to the concentration of the solute in the liquid. This equation is known as Freundlich adsorption isotherm as shown in Eq.(7)

$$q_e = K_F C_e^{1/n} \quad (7)$$

Where  $q_e$  and  $C_e$  have definitions as previously presented for the Langmuir isotherm.  $K_F$  is Freundlich adsorption constant and  $n$  is adsorption intensity. Again, the linear form of Freundlich Adsorption Isotherm is usually used to fit data as

$$\log q_e = \log K_F + \frac{1}{n} \log C_e \quad (8)$$

### 1.3 Review of literature

There are many reports about the preparation of hierarchical porous carbon materials as adsorbent, but their process use toxic chemical and multi-step processes such as:

Malekbala and coworkers (2015) prepared carbon coated monolith by dip-coating of furfuryl alcohol (FA) as a carbon source, Py as a binder and  $\text{HNO}_3$  as a catalyst. Triblock copolymer F127 was used as a mesopore templating. The preparation method was coated on the cordierite monoliths scaffold with the precursor. Finally, carbon coated monolith was obtained. The obtained material was used as an adsorbent for methylene blue (MB). This work studies effects of pH, salt, contact time, initial dye concentrations and temperature on dye adsorption. The maximum adsorption capacity was 388 mg/g. The recycle test showed that 82.1% performance (Malekbala, Khan et al. 2015).

Xia and coworkers (2015) prepared hierarchical porous carbon by using resol as a precursor, and triblock copolymer F127 as a soft-templating mesostructure onto the wood scaffold. This is indicate that the hydrogen bonding between the resol and the surface of the poplar. This work indicated that the mass ratio of the resol to poplar shavings have affect on the thickness of polymer. In addition, the obtained material showed high adsorption performance (Xia, Li et al. 2015).

Ghimbeu and coworkers (2014) prepared a ordered mesoporous carbon (OMC) by self-assembly of phloroglucinol/glyoxylic acid with template. Glyoxylic acid is used for a substituent of carcinogenic formaldehyde usually employed in a synthesis. Moreover, this method was simple, rapid and no catalyst. The researchers found that the affect of ratio between carbon precursor : template (F127) can control mesopore

structure. The prepared material exhibit high surface area, large pore volume and defined pore size. The synthesis methods, unfortunately pose disadvantages because carbon materials synthesized were only obtained in low amounts, making them difficult to be used for practical applications. (Matei Ghimbeu, Vidal et al. 2014).

Wang and coworkers (2011) prepared ordered mesoporous carbon (OMC) by organic-organic self-assembly method. Triblock copolymer Pluronic F127 were used as a template, phenolic resol as a carbon precursor and polyurethane foam as a scaffold. The effects of the concentration of resol on the mesostructure of the carbons was investigated. The prepared ordered mesoporous carbon showed high surface area and pore size diameter 4.5 nm. The composite has great electrochemical performance of about 130 F/g in KOH electrolyte. Unfortunately, it was evident that the use of the carcinogenic formaldehyde was a main drawback concerning the health issues. (Wang, Xue et al. 2011).

Hosseini and coworkers (2011) prepared carbon coated monoliths by surface coating of furfuryl resin on cordierite monoliths. Furfuryl resin was used as carbon precursor. Physical and chemical characteristics have been investigated. The surface of obtained material showed 65% of total pore volume falls in mesopore. When using as adsorbent for methyl orange removal, the maximum absorption capacity is 88.5 mg/g. The desorption of methyl orange was studied. Sodium hydroxide solution was used as eluent. The maximum recovery of methyl orange decrease after 3 cycles. (Hosseini, Khan et al. 2011)

Chen and coworkers (2017) prepared hierarchical porous carbon material from different biomass by two-step synthesis, carbonization under nitrogen and thermal oxidation in air. The mesopore and micropore increased after thermal oxidation. In addition, the thermal oxidation provided oxygen functional group lead to hydrophilic surface. The resulting materials were used as adsorbent to studies the correlations between pore size and adsorption performance. Its show that the adsorption behavior depend on pore size.

Elaigwa and coworkers (2014) prepared mesoporous carbon monoliths by self-assembly. This process used waste plant material as carbon source and F127 as a

template. The physical and chemical properties were studied. The material has a surface area of 219 m<sup>2</sup>/g and average pore size of 6.5 nm. This synthesis method is a simple, inexpensive and the obtained material can be applied to application such as adsorption, catalysis and electrochemistry (Elaiwu and Greenway 2014).

Chen and coworkers (2015) prepared mesoporous carbonaceous materials by evaporation induced self-assembly on the surface of cigarette filters. Phenol/formaldehyde resin used as a carbon precursor, triblock copolymer F127 as the template and cigarette filters as a scaffold. The adsorption of phenol and CO<sub>2</sub> was studied, the adsorption capacity were 261.7 mg/g and 2.48 mmol/g respectively. The resulting material showed good thermal stability (Chen, Li et al. 2015).

Huang and coworkers (2012) prepared hierarchically porous carbon material by surface coating and solvent evaporation-induced self assembly method. Phenol-formaldehyde resins were used as carbon precursor and sugarcane bagasse as the scaffold. This method used a carcinogenic formaldehyde was a main drawback. The monolithic carbon materials exhibited high specific surface area (487–544 m<sup>2</sup>/g) and good electrochemical property. (Huang and Doong 2012)

Hierarchically porous carbon materials prepared through the same self-assembly surface coating strategy have been used the macroporous scaffolds varied from different types of materials, such as cordierite, polyurethane foam cigarette filters and wood. However, a little number of reports presented the use of pure natural precursors as macroporous scaffolds. Despite some of them being used to study the adsorption performance. Moreover, most of them relied on the use of formaldehyde and their synthetic methods seemed to be complicated, resulting in time consuming, health and environmental concerns.

#### 1.4 Objectives

- To synthesize and characterize hierarchical porous carbons (HPCs) from sugarcane bagasse by self-assembly coating.



- To systematically investigate the influence of the pore texture and chemical properties on the adsorption properties of the HPCs towards dyes in terms of adsorption capacity and kinetics.

## CHAPTER 2

### EXPERIMENTAL

#### 2.1 Chemicals and materials

1. Triblock copolymer Pluronic F127 (poly(ethylene oxide)-block-poly(propylene oxide)-block-poly(ethylene oxide), PEO<sub>106</sub>PPO<sub>70</sub>-PEO<sub>106</sub>, Mw = 12,600 Da) was purchased from Sigma-Aldrich
2. Phloroglucinol (1,3,5-benzotriol, C<sub>6</sub>H<sub>6</sub>O<sub>3</sub>) was purchased from ACROS Organics
3. Glyoxylic acid monohydrate (C<sub>2</sub>H<sub>2</sub>O<sub>3</sub>•H<sub>2</sub>O) was purchased from Merck KGaA
4. Ethanol (99.5%, A.R., RCI Labscan)
5. Sugarcane bagasse (*Saccharum officinarum* L.) using as a scaffold, was acquired from agricultural plant in Lopburi, Thailand with approximately cellulose 40-50%, hemicellulose 25-35%, lignin 15-25% and a few quantities of inorganic element and wax (Sun et al., 2004).

#### 2.2 Equipment and instruments

1. Scanning electron microscopy (SEM, Quanta 400, FEI)
2. Field emission scanning electron microscope (FE-SEM, Apreo, FEI)
3. Transmission electron microscopy (TEM, JEOL JEM-2010)
4. Fourier transform infrared spectroscopy (FTIR, Spectrum GX, Perkin Elmer, US)
5. X-ray photoelectron spectroscopy (XPS, ULVAC-PHI, PHI 500 VersaProbe II using Al K $\alpha$  radiation from Thailand Synchrotron Light Research Institute)
6. N<sub>2</sub> adsorption-desorption analysis (Micromeritics, ASAP 2460)
7. Oven (UNE200, Memmert)
8. Tube Furnace (Carbolite)
9. Thermostat shaker water bath (Model WB/OB 7-45, WBU 45, Memmert)
10. UV-Vis spectrophotometer (UV 2600, Shimadzu)

## 2.3 Methods

### 2.3.1 Preparation of monolithic hierarchical porous carbon materials

Hierarchical porous carbon monolith were synthesized using the following procedure. First, the sugarcane bagasse was collected, washed with distilled water several times to remove dirt, impurity and residual sugar and then dried in an oven at 100°C for 48 h. The dried raw material was then cut into 0.5 × 1.0 × 0.2 cm pieces. The resulting monolith samples are here named BG. The average bulk density of the BG was 0.15 g/cm<sup>3</sup>. Their average macropore sizes (determined using SEM) were in the range of 10 - 100 μm. These macropores were originated from the natural xylem and phloem of raw bagasse.

For a typical preparation method of the hierarchical porous carbon composites, phloroglucinol (1.02 g), glyoxylic acid monohydrate (0.76 g) and Pluronic F127 (1.96 g) were dissolved under stirring at room temperature in absolute ethanol (50 mL) to obtain a clear yellowish solution. 4.0 g of dried BG was mixed with the above solution and the mixture was stirred for 30 min at 300 rpm in a foil-capped 250 mL beaker with a diameter of 7 cm. After that, to ensure the homogeneous mixing, the mixture was manually kneaded with a spatula every 30 min for 3 h. During this process, the solution amount in the container was gradually reduced until it was no longer present in the container, indicating that the precursor solution was adsorbed by the BG.

Subsequently, the BG monoliths wetted with the solution were divided and transferred into three Petri dishes, then dried at room temperature (RT, 30 ± 2 °C) for 10 h in order to evaporate the ethanol and induce self-assembly of the carbon precursor/F127 composite on the surfaces of BG. Then, a thermal treatment at 80 °C for 48 h was performed to cross-link the carbon precursor/F127. The obtained materials were pyrolyzed at 800 °C under a nitrogen (N<sub>2</sub>) atmosphere for 3 h in a tubular furnace. The heating rate from ambient temperature to 600 °C was 1 °C/min, and kept at 600 °C for 15 min. From 600 °C to 800 °C, the heating rate was 5 °C/min, and then holding at 800 °C for 3 h. The resulting sample was collected and then labeled “HPC(2.4)\_800” (HPC = Hierarchically Porous Carbon), “(2.4)” represents the mass ratio of the template (F127):phloroglucinol+glyoxylic acid, while “\_800” indicates

the pyrolysis temperature in degree Celsius. The mass ratio of F127:phoroglucinol+glyloxilic acid was varied to 1.2, while the other synthesis procedures remained the same. These samples are then here labeled “HPC(1.2)\_800”.

As a control experiment, BG was carbonized directly without the coating process and the sample was named “BG\_800”. The non-templating sample was prepared with the same procedure as for the HPC samples but without use of F127 template and was designated as “BG\_PGF\_800”.

All resulting porous carbon materials were collected and designated using the symbols shown above. In order to improve the surface area and porosity, 2 g of each sample after the carbonization at 800 °C was then heat-treated in a 3 × 15 cm boat crucible placed in a muffle furnace at 400 °C for 1 h in air. All the samples after carbonization at 800 °C and then heat-treated in air was designated using the above corresponding symbols followed by the letter “A”, for instance, HPC(2.4)\_800A.

In order to confirm the good reproducibility, the preparation of all the samples was replicated at least 3 times.

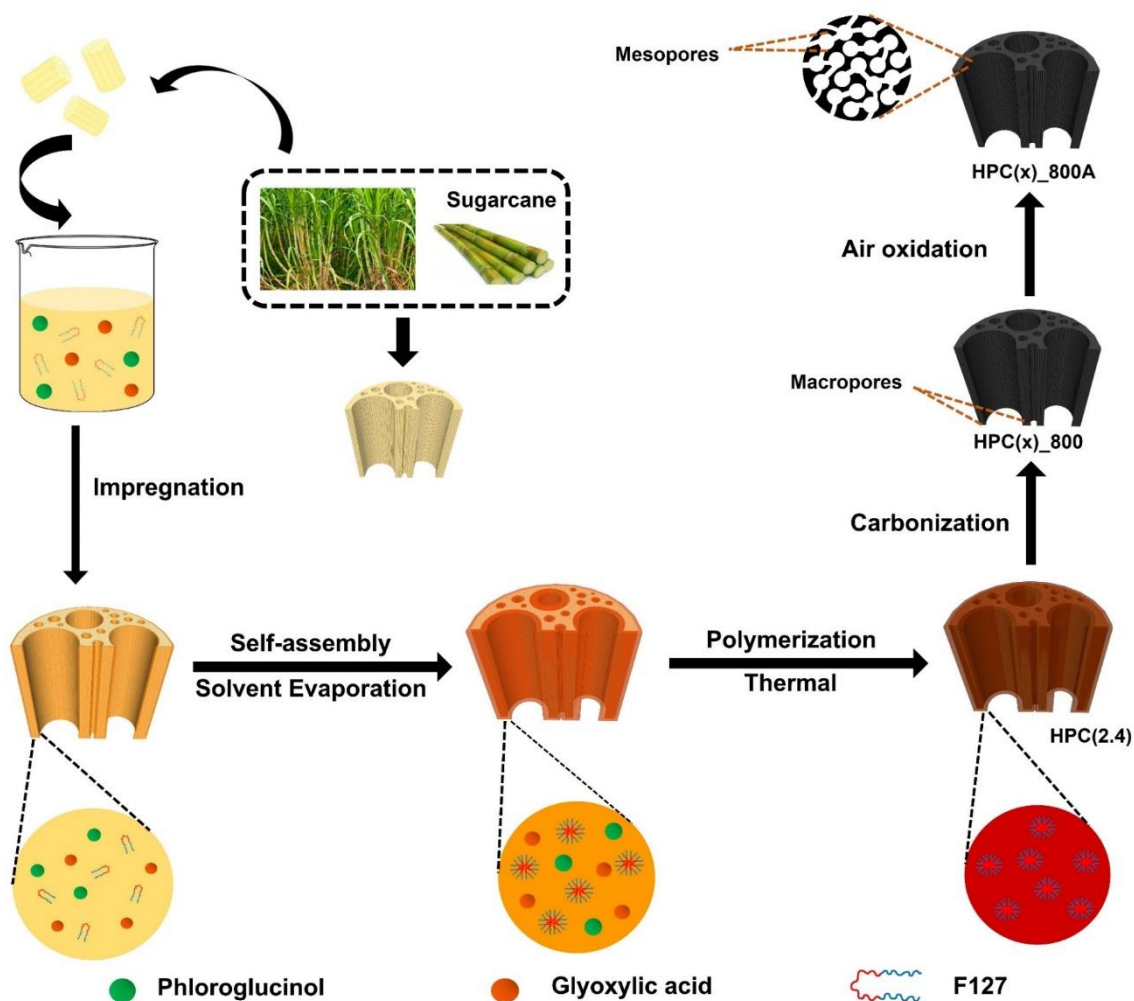


Figure 1 Schematic Illustration of the preparation steps for all HPC by Self-Assembly Methods.

### 2.3.2 Characterization of monolithic hierarchical porous carbon materials

1. Scanning electron microscopy (SEM) was used to study the surface and morphology of Hierarchical porous carbon materials.
2. Transmission electron microscopy (TEM) was used to study the pore texture of mesopore
3. Field emission scanning electron microscope (FE-SEM) was used to determine mesopore on the surface of Hierarchical porous carbon materials.
4. Fourier transform infrared spectroscopy (FTIR) was indicated the functional groups on the surface of samples. The FTIR spectra were obtained using KBr technique. The spectra were recorded from range  $4000 - 400 \text{ cm}^{-1}$ .

5. **X-ray photoelectron spectroscopy (XPS)** was used to analyze elemental composition and functional groups on the sample surfaces, both quantitatively and qualitatively.
6. **N<sub>2</sub> adsorption-desorption isotherm analysis** was performed at 77 K. The samples were degassed at 120 °C for 16 h before the measurements. From the sorption experiments, specific surface areas ( $S_{\text{BET}}$ ) were determined using Brauner-Emmett-Teller (BET), total pore volume is evaluated at  $p/p_0$  of 0.95-0.97, micropore area and volume were evaluated using t-plot method and density functional theory (DFT model). The pore size distribution in both micropore and mesopore regions, as well as the average mesopore size was determined using the DFT and Barrett-Joyner-Halenda (BJH) models, respectively. The samples were subject to the measurements in the monolithic form without being ground as can be seen in Figure.2. An analysis tube was filled with 30-100 mg of the sample. At least three replicated measurements using samples prepared from different lots were performed. We found only slightly different results by using different weights and lots of the same sample. This confirmed the reproducibility of our synthesis procedures.



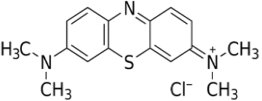
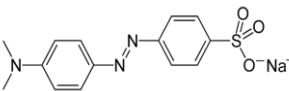
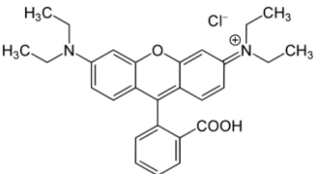
**Figure 2** Photograph of the samples contained analysis tube without being ground.

### 2.3.3 Adsorption studies

#### 2.3.3.1 Adsorption Kinetics

The batch adsorption studies employed 3 dyes, including methylene blue (MB) (representing a cationic dye), methyl orange (MO) (representing an anionic dye) and Rhodamine B (RhB), representing a large molecular-weight dye. Their chemical structures and properties are shown in Table.1.

The kinetic adsorption were carried out by 30 mg of the carbon materials in 50 mL conical flasks of 40 mg/L dye solution, on a thermostat shaker water bath (Model WB/OB 7-45, WBU 45, Memmert) at  $30 \pm 2$  °C, at the natural (unadjusted) pH of 6.8, for 0-96 h duration.

Dye	Chemical structure	Molecular size (nm)	Molecular weight (g/mol)	$\lambda_{\max}$ (nm)	Charge
Methylene blue (MB)		1.70×0.76×0.33	319.85	644	Positive
Methyl orange (MO)		1.31×0.55×0.18	327	465	Negative
Rhodamine B (RhB)		1.59×1.18×0.56	478	554	Positive

**Table 1.** Chemical structure, Molecular size, Molecular weight,  $\lambda_{\max}$  of UV/Visible adsorption for dyes.

### 2.3.3.2 Adsorption isotherm

The adsorption isotherms were studied in 50 mL vials with 0.03 g of the hierarchical porous carbon materials and 25 mL of 0-850 mg/L dye solutions. The mixture was shaken for more than 48 h at  $30 \pm 2$  °C, at the natural pH of 6.8.

After adsorption, the solution was easily separated from the mixture without either centrifugation or filtration, and then was used for further measurements of dye concentrations. The concentrations of dye before and after adsorption were determined by a calibration method, using a UV-Vis spectrophotometer. The wavenumbers (**V**) for the detection of the dyes are listed in Table 1. The adsorbed amount of dye was calculated with Eq. (1) as follows

$$q_e = \frac{(C_0 - C_e)V}{m}$$

where  $C_0$  and  $C_e$  are the concentration of dye before and after adsorption (mg/L),  $m$  is amount of the adsorbent (g), and  $V$  is volume of the dye solution (L).

### 2.3.3.3 Adsorbent regeneration

For recycling tests, Adsorbent adsorb methylene blue 100 ppm with 25 mL by 0.03 g of HPC(2.4)\_800A for 48 hour at room temperature. Adsorbent after methylene blue adsorption was regeneration in tube furnace under  $N_2$  atmosphere at 500°C only for 1h with a heating rate of 5°C/min. The adsorbent was subjected to 3 consecutive adsorption-desorption cycles. The adsorption efficiencies are normalized so that  $q_e$  of the first adsorption cycle is 100%.



## CHAPTER 3

## RESULTS AND DISCUSSION

## 3.1 Formation of hierarchical porous structures

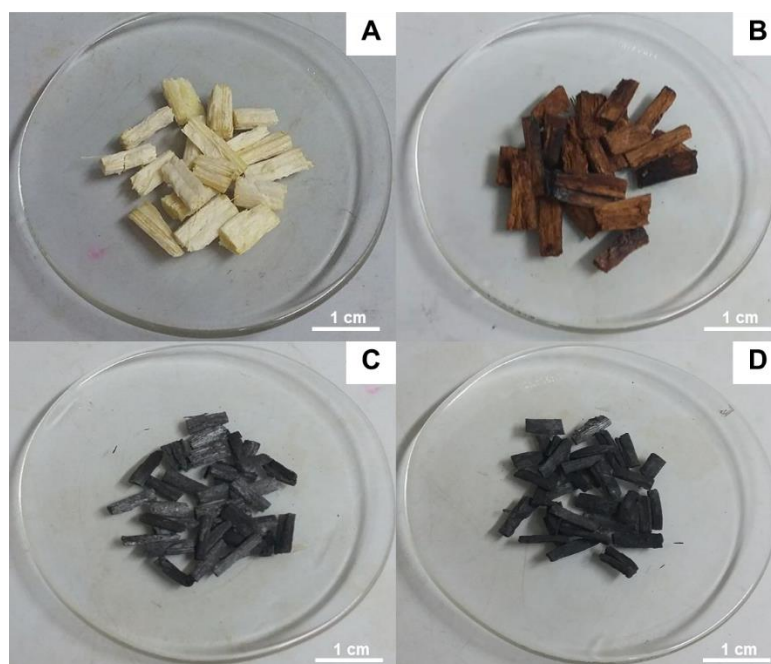


**Figure 3** Optical images of (A) Sugarcane Bagasse(BG), (B) Composite HPC(2.4), (C) HPC(2.4)\_800 and (D) HPC(2.4)\_800A.

The preparation method introduced in this work is considered simple and suitable for large scale synthesis of monolithic HPCs. The use of toxic chemicals reported in many previous works for example, evaporated formaldehyde and even activating agents ( $\text{ZnCl}_2$ ,  $\text{KOH}$ ,  $\text{H}_3\text{PO}_4$ ) can be avoided in the present work. Furthermore, binders and freeze drying step generally employed to synthesize a monolithic shape was no longer needed.

In the first step, simply mixing phloroglucinol, glyoxylic acid, and triblock copolymer F127 in ethanol resulted in a homogeneous clear yellow solution. Then, BG pieces were introduced into the mixture solution and the mixture was stirred for

30 min. Upon mixing the solution and BG as a scaffold material, the morphological structure of BG with open macroporosity allows for the facile penetration of the carbon precursor (phloroglucinol, glyoxylic acid and F127 mixture) into the inner pore spaces by the capillary force, as well as for deposition of the precursor on the outside surfaces. The incorporation of solution precursors occurs onto electron-rich oxygen atoms of the polar hydroxyl/ether groups in cellulose through hydrogen bond interactions. During this step, the color of BG specimens became darker and wettability throughout all the specimens was also observed, further confirming the introduction of the precursor solution into the cellular channels of BG. The subsequent evaporation of the solvent (ethanol) induced further coating of the carbon precursor and initiated the self-assembly of phloroglucinol/glyoxylic acid phenolic resins around the F127 template through the formation of micelles of F127. Consequently, upon the solvent evaporation, the micelles were surrounded by and interact with carbon precursors via hydrogen bonds. This step is underlined as “evaporation self-assembly (EISA)”, and has been employed to synthesize nanoporous and nanostructure materials in the form of both powder and film.

Next, the obtained material was subjected to a further thermal treatment at 80 °C for 48 h in order to complete the cross-link process between glyoxylic acid and phloroglucinol. This resulted in a change of material's color from dark yellow to reddish brown, as well as hardened the monolithic specimens (Figure 3.). The complete carbonization at 800 °C turned the materials into monolithic porous carbon and completely removed the template, leaving the mesopores on the sugarcane scaffold. The complete absence of the F127 template also occurred in the carbonization process. This resulted in the formation of mesoporous structure and converted the carbon precursor and BG into carbon matrix. Although the resulting black carbon monolith HPC shrunk by ~75 %V in comparison with the BG scaffold, they retained the monolithic characters with sufficient strength (Figure 3.). We noted that even after the heat treatment in air at 400 °C for 1 h, the monoliths were well retained with only tiny weight loss (~2 wt%). It should also be noted that the carbonized monolith and the monolith after air treatment showed the similar

appearance characteristics. The characteristics of all the prepared samples show similar physical appearance.

### 3.2 Characterization of hierarchical porous structures

To investigate the morphology of the samples, SEM was employed. The SEM images of pristine sugarcane bagasse (BG) and the monolithic HPC (HPC(2.4)\_800A) are shown in Figure 4A. and Figure 4B., respectively. Both samples similarly possess the macropores originated from the natural xylem and phloem of raw bagasse. Determination of the decrease in the macropore sizes was nevertheless difficult because the macropore size distribution of the raw bagasse was rather broad (50-110  $\mu\text{m}$ ). Nevertheless, the retained macropores indicate that the surface coating, pyrolysis at 800 °C and subsequent air treatment at 400 °C had no effect on the changes in the macropore morphology of the raw bagasse. Closer looks using images from the high resolution field emission SEM (FE-SEM) (Figure 4D-E) on HPC(2.4)\_800A reveal that mesopores were present on the scaffold surfaces. Importantly, the presence of both macropores and mesopores results in a hierarchically porous structure of the resulting materials. In general, the macropores may improve the diffusion performance of adsorbates into the inner pores, while the mesopores act as active adsorption sites. The TEM images of HPC(2.4)\_800A (Figure 4F-G) further confirmed the existence of mesopores. Different pore morphologies can be observed in this sample, combining the disordered mesopores (Figure 4F) with the tube-like pore structure (Figure 4G); however, both types of pores had the same average pore diameter of ~6 nm (Figure 4F and Figure 4G).

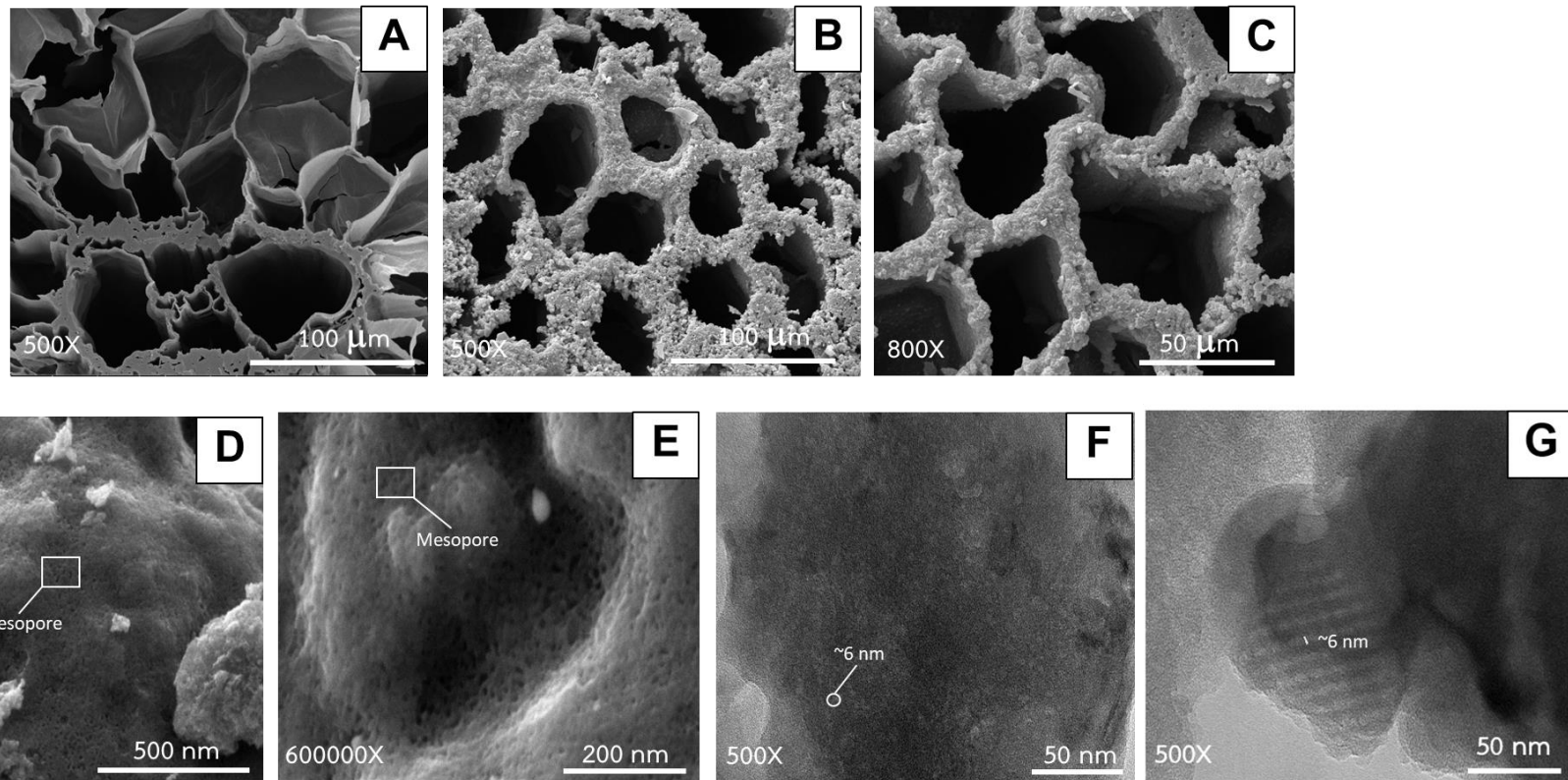


**Figure 4** SEM and TEM analysis. (A) SEM image at 500x of sugarcane bagasse (sectional areas of the vessels), (B-C) SEM images at 500x-800x of HPC(2.4)\_800A (sectional areas of the vessels), (D-E) FE-SEM image at 300000x-600000x of HPC(2.4)\_800A and (F-G) TEM image at 500x of HPC(2.4)\_800A.

To further confirm the existence of the templated mesopores and investigate BET surface area, porosity and pore size distribution, N<sub>2</sub> sorption analysis was performed and the results are shown in Figure 5. The N<sub>2</sub> sorption isotherms of all samples prepared via the templating technique (HPC series before air oxidation) exhibit a type IV isotherm according to IUPAC with a distinct hysteresis loop, indicating that the mesoporosity contributes to the main fraction of all pore texture in material structure. The Table. 2 shows the pore textural properties from N<sub>2</sub> sorption experiments. The BET surface areas for all samples are in the range of 400-600 m<sup>2</sup>/g. The mesopore volumes of the series of HPCs samples were in range of 0.13-0.25 cm<sup>3</sup>/g, contributing to 45-60 V% of the total pore volumes. Moreover, the dominant mesopore sizes were in the range of 5.3-5.5 nm, as clearly observed from BJH pore size distributions (Figure 6, Table. 2). The mesopore sizes agree well with the TEM results. The observed mesopore sizes correspond well to a typical size of F127 micelles, (REF Chuencheom) further indicating the successful templating.

Mesopore surface areas of HPC(1.2)<sub>800</sub> and HPC(2.4)<sub>800</sub> exceed 100 m<sup>2</sup>/g, which is considerably high compared to those of conventional microporous activated carbons.

In a sharp contrast, BG-800 and BG\_PGF\_800, which both are the non-templating samples show typical isotherms of type I, suggesting that most of pore size is dominated by microporosity (pore size < 2 nm) for these two non-templated samples. Moreover, both BG\_800 and BG\_PGF\_800 show no mesopore contribution in the mesopore region (Figure 6).

The origin of microporosity for both the samples is probably from the intrinsic porosity generated from the decomposition of small molecules of the starting materials, generally composed of large fractions of cellulose and hemi-cellulose (BG-800) and the resin polymer in case of BG-PGF-800.

Micropore size distribution was studied by NLDFT model and is shown in Figure 6. All the samples before air oxidation exhibit small micropores with an average diameter of 0.8 nm.

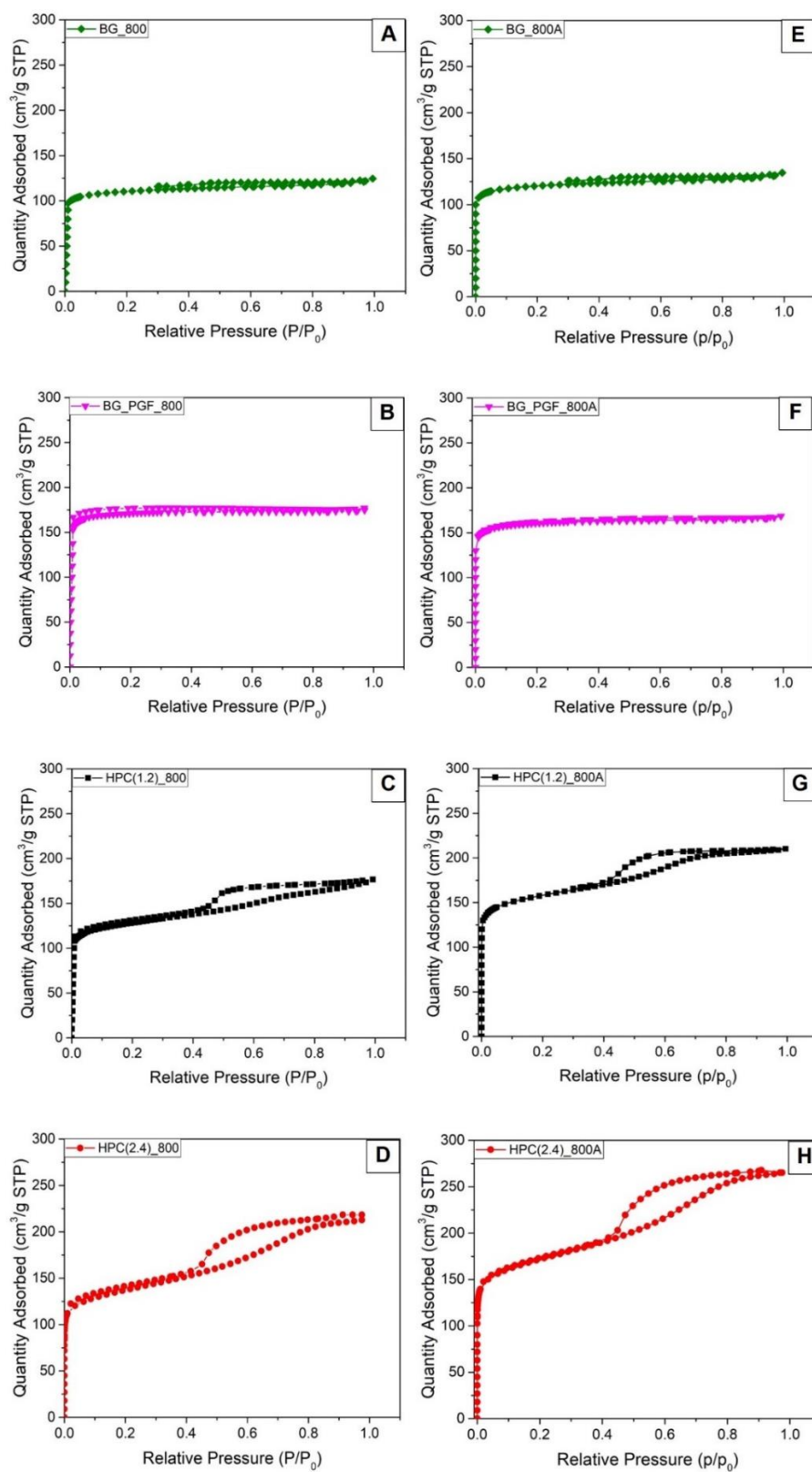


**Figure 5** Nitrogen adsorption-desorption isotherm of (A-D) samples before air oxidation, (E-H) samples after air oxidation.

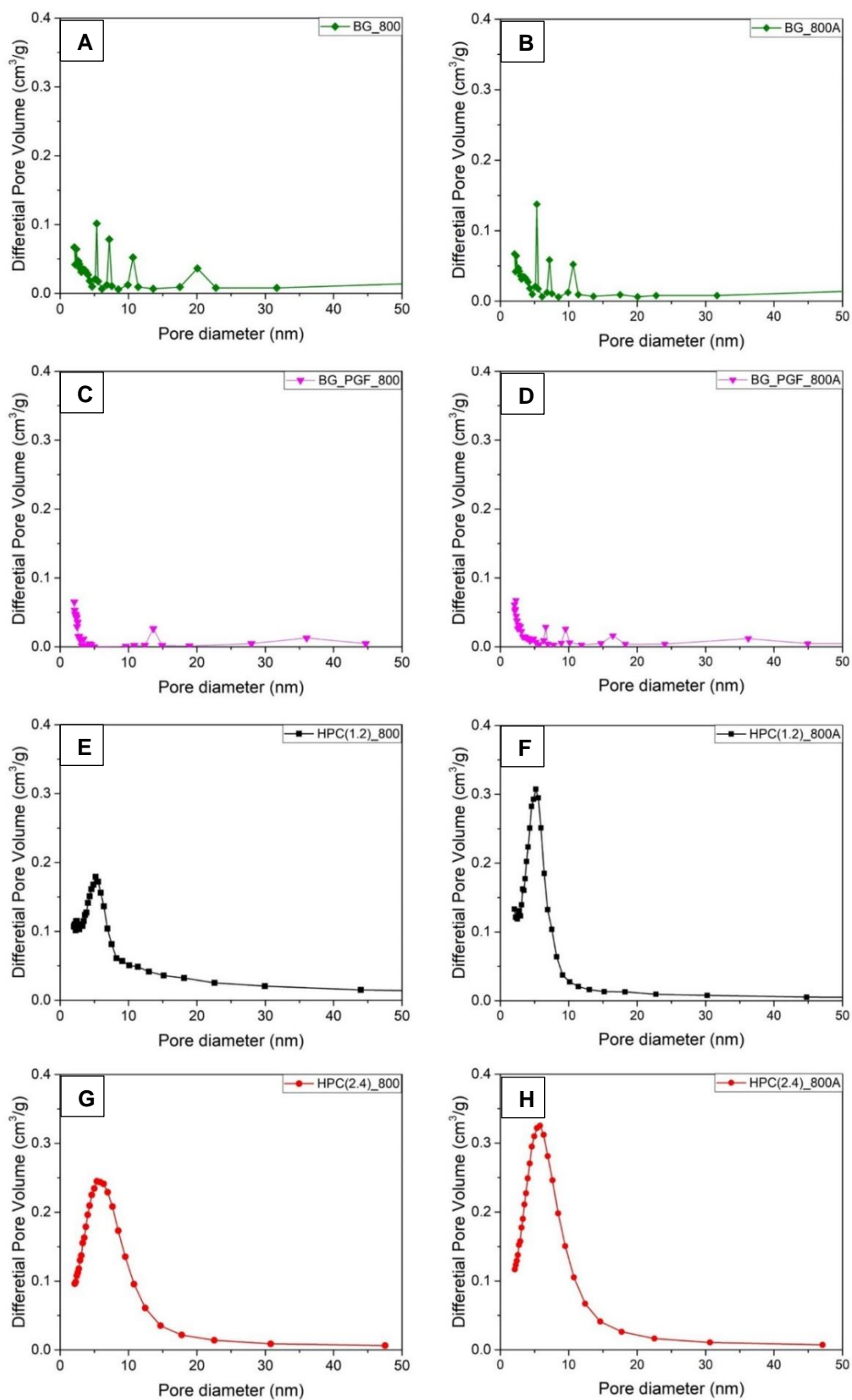


Figure 6 Mesopore size distribution using BJH model of all samples.

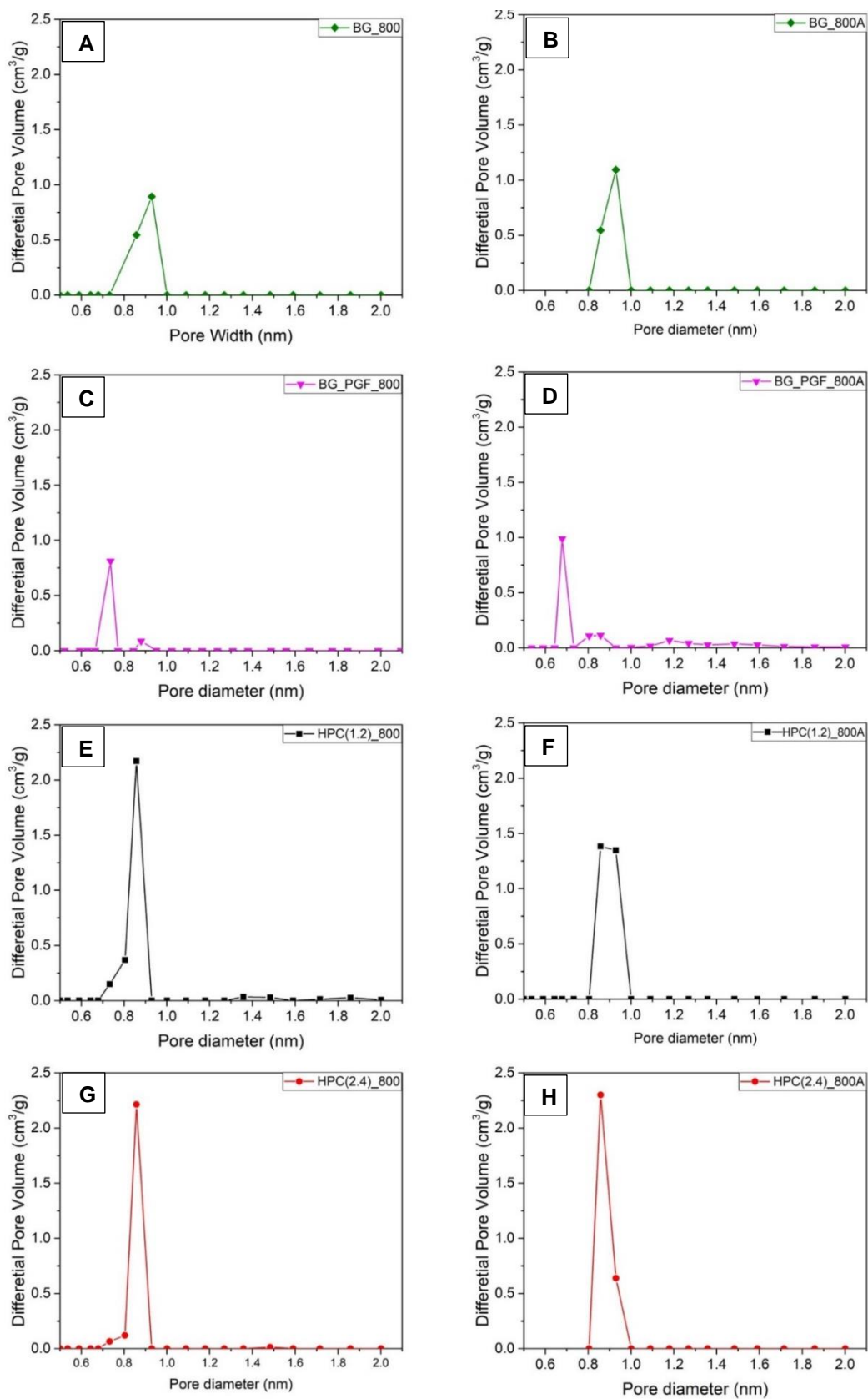


Figure 7 Micropore size calculated by DFT method of all samples.



Samples	Template/ Carbon precursors	Surface area (m <sup>2</sup> /g)			Pore Volume (cm <sup>3</sup> /g)			% Mesopore <sup>f</sup>	Pore size (nm)	
		BET	Micro <sup>a</sup>	Meso <sup>b</sup>	Total <sup>c</sup>	Micro <sup>d</sup>	Meso <sup>e</sup>		BJH <sup>g</sup>	DFT <sup>h</sup>
BG_800	0	421.60 ± 48.13	384.24 ± 39.05	37.36 ± 9.08	0.180 ± 0.028	0.150 ± 0.021	0.030 ± 0.007	16.67	-	0.89
BG_800A		476.79 ± 51.85	416.13 ± 37.49	60.66 ± 14.36	0.210 ± 0.034	0.159 ± 0.026	0.051 ± 0.008	24.29	-	0.93
BG_PGF_800	0	618.56 ± 61.24	575.36 ± 53.89	43.20 ± 7.35	0.269 ± 0.034	0.224 ± 0.025	0.045 ± 0.009	16.61	-	0.81
BG_PGF_800A		638.78 ± 57.36	584.78 ± 49.58	54.00 ± 7.78	0.257 ± 0.033	0.224 ± 0.023	0.033 ± 0.010	12.73	-	0.68
HPC(1.2)_800	1.2	492.76 ± 62.58	367.56 ± 43.29	125.21 ± 19.29	0.273 ± 0.027	0.143 ± 0.019	0.130 ± 0.008	47.48	5.5	0.86
HPC(1.2)_800A		606.49 ± 49.96	448.61 ± 39.11	157.87 ± 10.85	0.325 ± 0.033	0.175 ± 0.022	0.150 ± 0.011	46.05	5.5	0.89
HPC(2.4)_800	2.4	514.00 ± 53.78	332.36 ± 34.12	181.64 ± 19.66	0.329 ± 0.025	0.133 ± 0.018	0.196 ± 0.007	59.64	5.4	0.86
HPC(2.4)_800A		644.01 ± 57.25	415.29 ± 42.08	228.72 ± 15.17	0.410 ± 0.032	0.165 ± 0.019	0.245 ± 0.013	59.65	5.4	0.86

<sup>a</sup> t-plot micropore area

<sup>b</sup> t-plot external surface area

<sup>c</sup> total pore volume

<sup>d</sup> t-plot micropore volume

<sup>e</sup> difference of total pore volume and micropore volume

<sup>f</sup> BJH adsorption average pore diameter

<sup>g</sup> DFT pore size

**Table 2** Detail textural properties measured by nitrogen sorption at 77K.

FTIR spectroscopy was used to provide information on the chemical functionalities of all samples qualitatively. Figure 8 reveal the FTIR spectra and Table. 3 details the band assignments. All samples before pyrolysis (BG, BG-PGF, HPC(1.2), HPC(2.4)) shows abundant oxygenated functional groups in FTIR spectra. All the characteristic bands of BG also appear in the spectra of HPC(1.2) and HPC(2.4). Furthermore, the bands at 2935 and 1157  $\text{cm}^{-1}$  are attributed to the C-H and C-O-C asymmetric stretching vibration of F127, while the bands around 2800 and 1850  $\text{cm}^{-1}$  are due to CH saturated bond of resin bridges and C=O in anhydrides. This observation indicates that the phloroglucinol/glyoxylic acid resin and F127 have been coated onto scaffold. All these bands disappeared after pyrolysis, including the F127 characteristic bands indicated that the F127 template was completely removed (HPC(1.2)-800 and HPC(2.4)-800). Furthermore, the presence of C=C peak was observed at 1700-1500  $\text{cm}^{-1}$  for all samples after pyrolysis. The presence of C=C band suggests that carbonization process converted resin and bagasse into carbon matrix. The spectra for all the pyrolysed samples and the ones after the air treatment show very similar patterns, suggesting that the air oxidation has no effect on the functional groups of the pyrolysed samples.

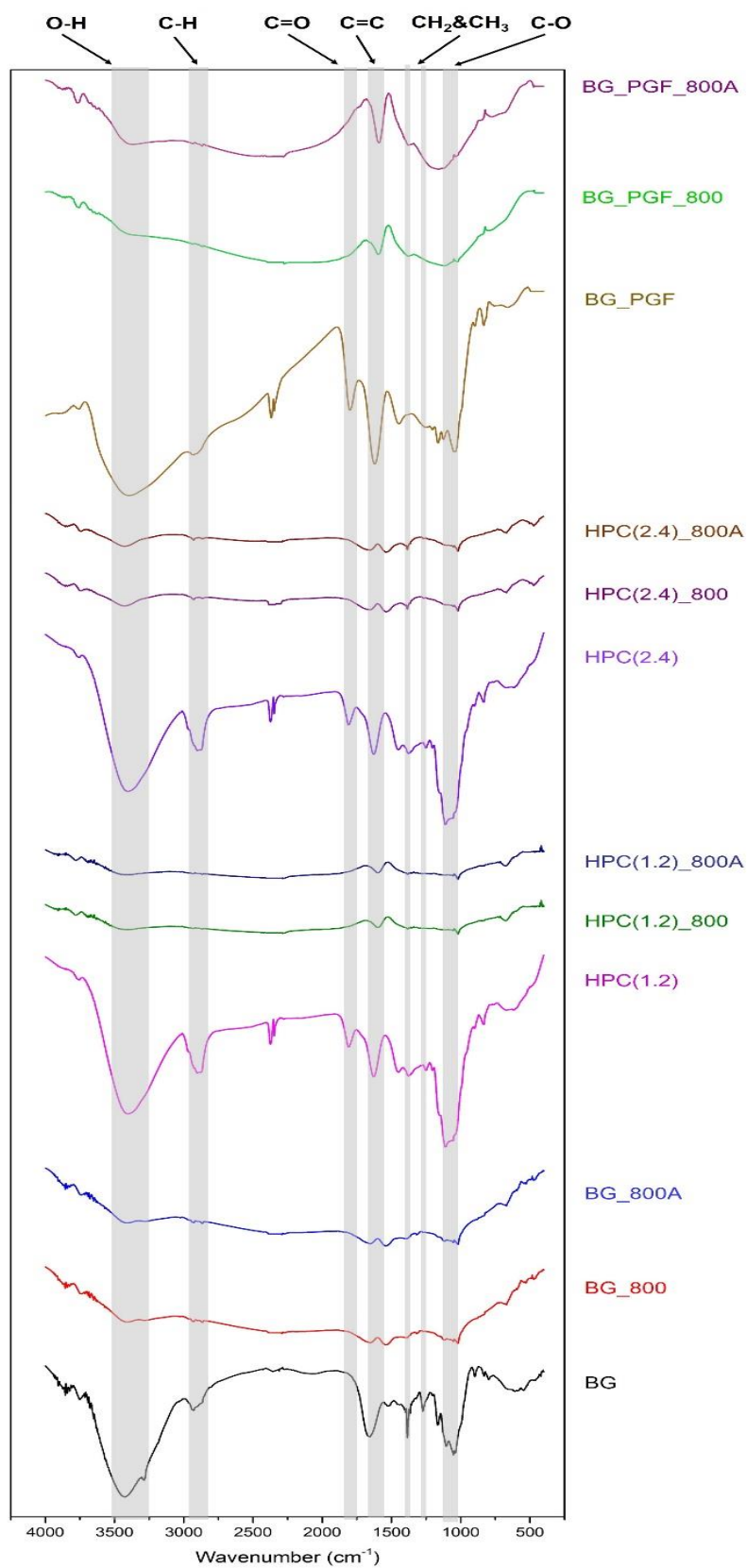


Figure 8 Functional group from FTIR spectrum of all samples.

Wave no.(cm <sup>-1</sup> )	Assignment	Structures
3600-3000	Stretching O-H	Hydroxyl, Carboxylic acid
3000-2800	Stretching C-H	Aliphatic, olefinic and aromatic hydrocarbons
1840-1800, 1780-1740	C=O anhydride	Cyclic actones and anhydrides
1700-1500	Stretching C=C or C=O	Olefinic, aromatic hydrocarbons, carbonyl
1430-1360	Bending O-H, C-H	Hydroxyl, Carboxylic acid olefins, methyl
1300-1000	Stretching C-O	Hydroxyl, ether

**Table 3.** Assignment of peak in FTIR of samples.

XPS analysis was carried out to determine elemental compositions and functionality assignments on the surface of samples. As can be seen in wide scan XPS in Figure 9, the presence of C 1s and O 1s peaks can be calculated to weight percentages of each element as shown in Table. 4. The carbon and oxygen contents in carbonized samples both before and after the air treatment were found to be in the ranges of ~85-91 wt% and ~8-15 wt%, respectively. This suggests that all those samples possessed high carbon content.

The deconvoluted spectra for C 1s and O 1s for HPC(2.4)\_800 and HPC(2.4)\_800A (Figure 10) show the similar XPS patterns at binding energies of 284.4 and 285.6 eV corresponding to C=C (with a large contribution) and C-O, respectively for C 1s. In high resolution O 1s spectra, the main oxygenated functional groups for these samples were found to be carbonyl and ether groups with binding energies of 530.9 and 530.2 eV, respectively. This confirms no significant change for functional groups on the surface between the samples before and after air oxidation, which agrees well with FTIR results. In addition, it is interesting to note that acidic oxygenated functional groups (carboxyl) are absent in the samples both after pyrolysis and air

oxidation process. All the samples were then found to possess non-acidic character. This neutral character of all the materials agrees with their  $\text{pH}_{\text{pzc}}$  values of  $\sim 6.5$  determined by pH drift method. This neutral charge is a typical behavior of carbon materials with large fraction of  $\text{sp}^2$  (C=C) character.

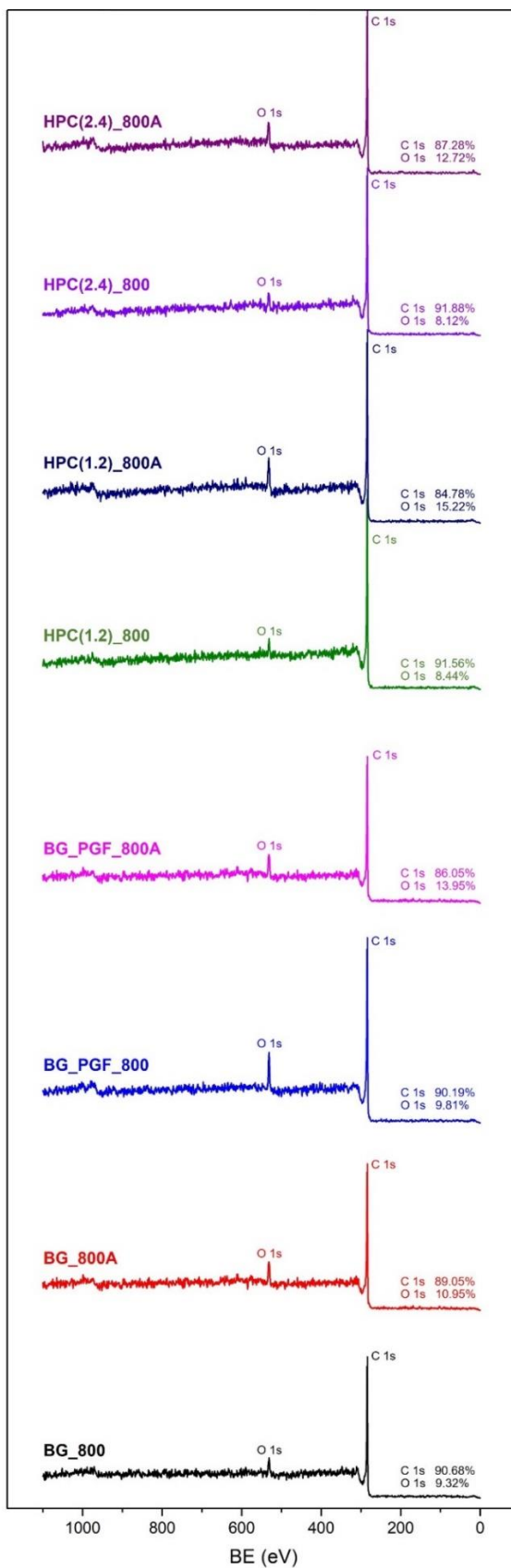


Figure 9 Survey spectrum from XPS of all samples.

Samples	%C		%O	
	by atomic	by weight	by atomic	by weight
BG_800	92.84	90.68	7.16	9.32
BG_800A	91.55	89.05	8.45	10.95
BG_PGF_800	92.45	90.19	7.55	9.81
BG_PGF_800A	89.15	86.05	10.85	13.95
HPC(1.2)_800	89.93	91.56	10.07	8.44
HPC(1.2)_800A	88.12	84.78	11.88	15.22
HPC(2.4)_800	93.78	91.88	6.22	8.12
HPC(2.4)_800A	90.14	87.28	9.86	12.72

**Table 4** The percentage compositions from XPS of all samples

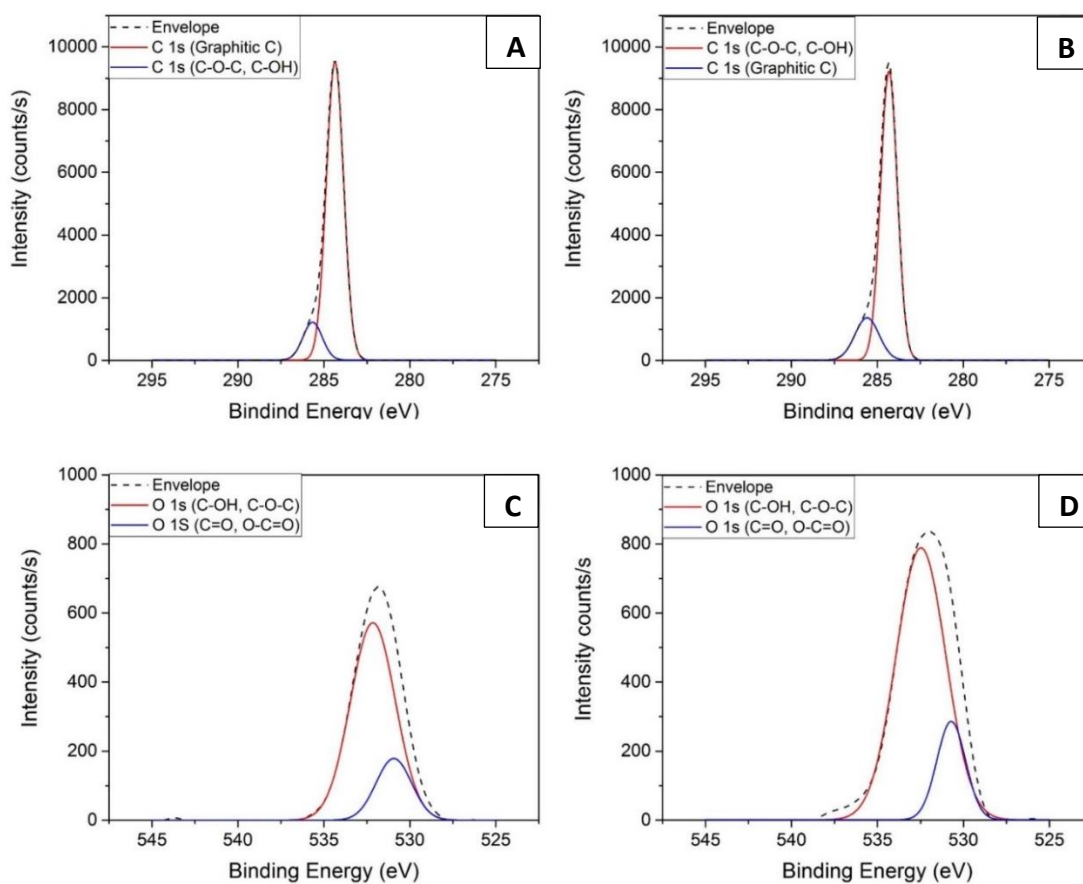


Figure 10 High-resolution XPS spectra of (A) C1s of HPC(2.4)\_800, (B) C1s of HPC(2.4)\_800A, (C) O1s of HPC(2.4)\_800 and (D) O1s of HPC(2.4)\_800A.



Peak	HPC(2.4)_800				HPC(2.4)_800A				Peak
	BE (eV)	%Weight	Area	%Area	BE (eV)	%Weight	Area	%Area	
C 1s	284.4	91.88	11945.7	87.5	284.3	87.28	11228.2	82.6	Graphitic C
	285.7		1702.2	12.5	285.6		2367	17.4	C-O-C/C-OH
O 1s	530.9	8.12	461.7	19.8	530.7	12.72	595.8	17.3	C=O/O-C=O
	532.2		1868.2	80.2	532.5		2853.7	82.7	C-OH/C-O-C*

**Table 5** Assignment of peak from XPS (C 1s and O 1s) for HPC(2.4)\_800 and HPC(2.4)\_800A.

### 3.3 Adsorption of dye by hierarchical porous carbon materials

#### 3.3.1 Adsorption kinetics of methylene blue by hierarchical porous carbon materials

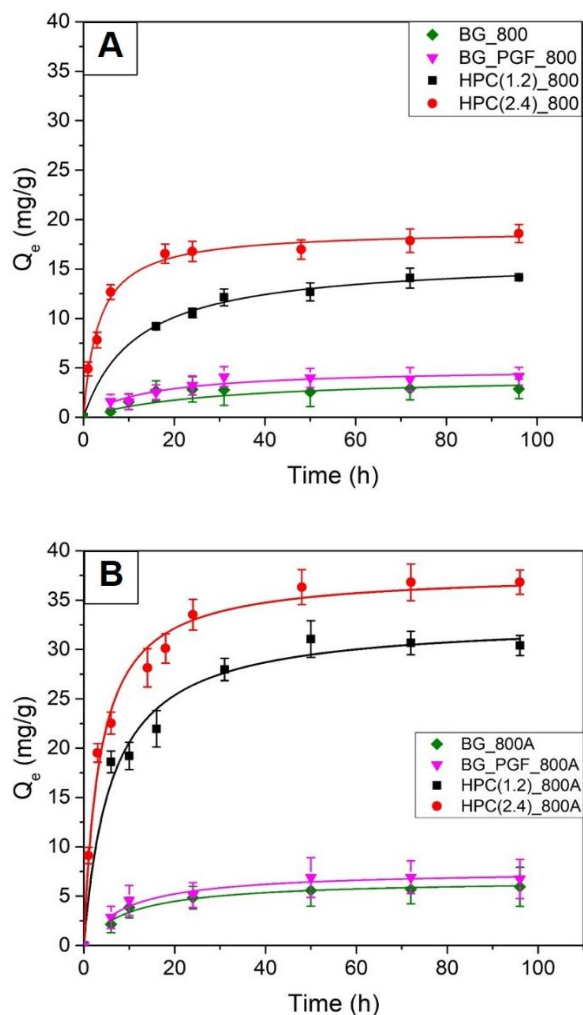


**Figure 11** Effect of contact time on the methylene blue adsorption over (A) All samples before air oxidation and (B) All samples after air oxidation. Reaction conditions: Initial concentration 40 ppm, temperature  $30\pm 2^\circ\text{C}$  and adsorbent dosage 0.03 g/25 mL.

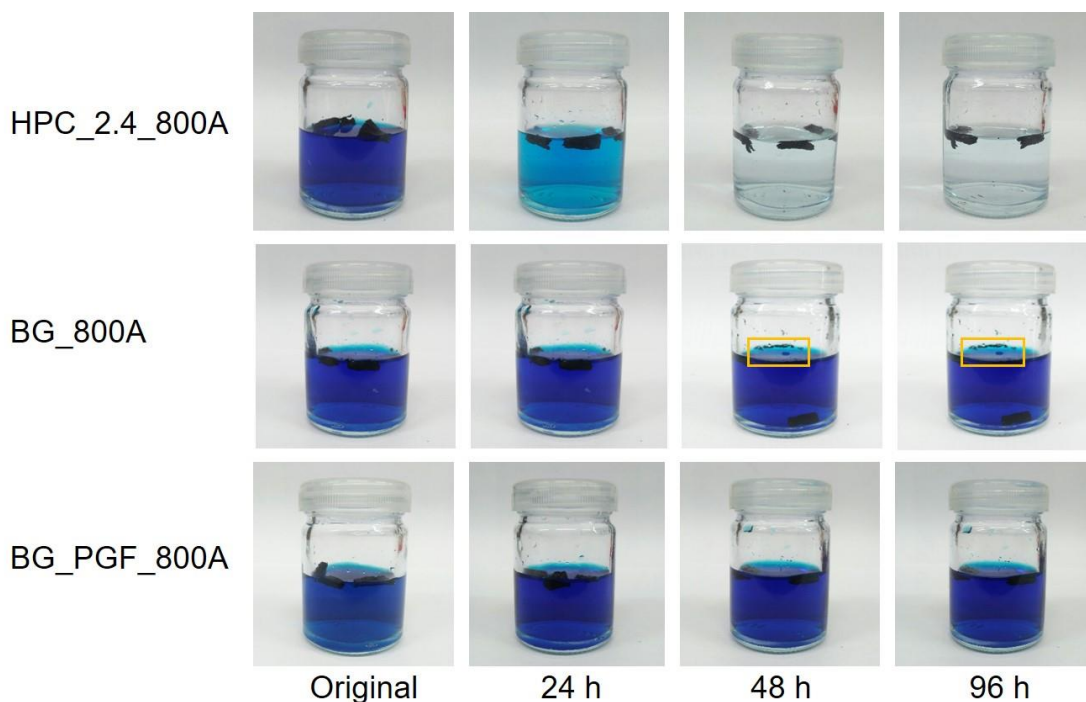


**Figure 12** Photographs of MB solution after adsorption by HPC(2.4)\_800A and MB adsorption by BG\_800A and BG\_PGF\_800A as a control.

Figure 12 and Figure 11 presents the change in MB color appearance and kinetic plots on MB adsorption, respectively by the adsorbents and with 40 mg/L MB initial concentration.

The adsorption capacities after reaching equilibrium for all the materials are in the order HPC(2.4)\_800A > HPC(1.2)\_800A > HPC(2.4)\_800 > HPC(1.2)\_800 > BG\_PGF\_800A > BG\_800A > BG\_PGF\_800 > BG\_800. It is obvious that all the non-templated samples show negligible adsorption capacity of < 8 mg/g.

It is interesting to note from Figure 12 that the MB solution became more colorless in 48 h for HPC(2.4)-800A. In other word, HPC(2.4)\_800A can quickly adsorbed MB more than 60% within 6 h and reached its equilibrium within 48 h. In addition, the monolith character of HPC(2.4)-800A can be retained even after 96 h, proving its strong mechanical stability. On the contrary, although BG-800A and BG-PGF-800A possessed higher SBET than HPC(2.4)-800, they showed almost no change in solution color even

after adsorption for 96 h. The fragile BG\_800A could not even reserve its monolith shape. Therefore, the good mechanical stability of the monolith HPC(2.4)\_800A is probably due to the strengthening of coated resin.

Also, it is noticeable that HPC(2.4)\_800A monoliths still floated on the water surface due to its low density (0.019-0.025 g/m<sup>2</sup>) after complete adsorption at 96 h. This behavior allows one to easily collect the adsorbent after the complete adsorption, making the sedimentation of the powdery adsorbents unnecessary.

We ground HPC(2.4)\_800A into a powder, and found that its adsorption of MB reached equilibrium faster than the monolith counterpart (12 h). However, the capacities of MB adsorption between the ground and monolith HPC(2.4)\_800A were the same (100 mg/g). This finding proves that despite its monolith feature, the active pores of HPC(2.4)\_800A function well, allowing full accessibility of MB molecules.

The detailed evaluation of the kinetics of MB adsorption is explained by fitting the kinetic data with a pseudo-second-order model (Table. 6-7).

In addition to higher adsorption capacities at equilibrium, the pseudo-second-order rate constants ( $k_2$ ) of the HPC series are obviously higher than those of non-templated ones. (Table. 6-7)

Samples	pseudo second-order		
	$q_{e,cal}$ (mg/g)	$k_2$ (g/mg·min)	$R^2$
BG_800	4.18	0.00851	0.80915
BG_PGF_800	4.98	0.01397	0.89806
HPC(1.2)_800	16.07	0.00529	0.99592
HPC(2.4)_800	18.93	0.001572	0.99080

**Table 6** Fitted parameters in the pseudo second order model for methylene blue 40 mg/g onto samples before air oxidation.

Samples	pseudo second-order		
	$q_{e,cal}$ (mg/g)	$k_2$ (g/mg·min)	$R^2$
BG_800A	6.67	0.01526	0.93424
BG_PGF_800A	7.62	0.01426	0.93638
HPC(1.2)_800A	33.04	0.00499	0.97899
HPC(2.4)_800A	37.80	0.00751	0.98777

**Table 7** Fitted parameters in the pseudo second order model for methylene blue 40 mg/g onto samples after air oxidation.

$k_2$  was found to be  $7.51 \times 10^{-3} \text{ g mg}^{-1} \text{ min}^{-1}$  for HPC(2.4)\_800A . This rate constant found in the present study is relatively comparable to those of other monolithic adsorbents reported in the literature under similar conditions. This is probably due to the hierarchical structure of the material, in which macropores allow fast diffusion of the bulky MB molecules to the active adsorption sites

### 3.3.2 Adsorption isotherm of methylene blue by hierarchical porous carbon materials

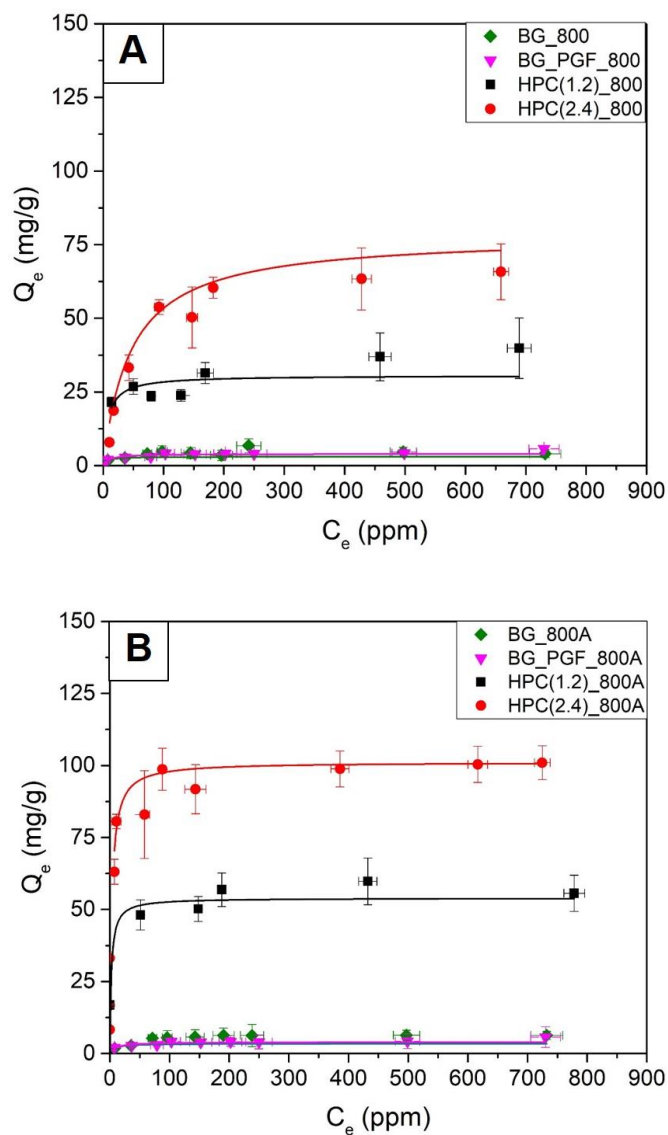


**Figure 13** Adsorption isotherm of methylene blue onto all monolith (A) All samples before air oxidation and (B) All samples after air oxidation. Reaction conditions: initial concentration 40-850 mg/g, temperature  $30 \pm 2^\circ\text{C}$  and adsorbent dosage 0.03 g/25 mL.

The adsorption isotherm of MB adsorption by all the materials is shown in Figure 13. The isotherm was well fit by the well-known Langmuir model. The details of fitted parameters and the non-linear form of Langmuir isotherm are explained in

Table. 8-9 in the Supporting Information. Maximum capacity from Langmuir model ( $q_m$ ) was a direct measure of the adsorption ability at equilibrium for an adsorbent.  $q_m$  values for MB adsorption follow the order HPC(2.4)\_800A > HPC(2.4)\_800 > HPC(1.2)\_800A > HPC(1.2)\_800 > BG\_PGF\_800A > BG\_PGF\_800 > BG\_800A > BG\_800 . This order is similar to the trend for adsorption maxima obtained in the kinetic study.

It is clear that HPC(2.4)\_800A show the best adsorption capacity (100.97 mg/g), while the  $q_m$  values are very negligible (< 4 mg/g) for all the non-template materials.

Samples	Langmuir parameters			$q_{\max, \text{exp}}$ (mg/g)
	$q_m$	K	$R^2$	
BG_800	3.04	0.17148	0.99100	4.05
BG_PGF_800	4.00	0.09961	0.99580	5.70
HPC(1.2)_800	30.64	0.12606	0.99991	39.83
HPC(2.4)_800	78.22	0.02153	0.99970	65.80

**Table 8** Fitted parameters values in Langmuir adsorption isotherm for methylene blue adsorption onto samples before air oxidation.

Samples	Langmuir parameters			$q_{\max, \text{exp}}$ (mg/g)
	$q_m$	K	$R^2$	
BG_800A	3.44	0.1439	0.99730	6.20
BG_PGF_800A	4.00	0.09961	0.99580	4.30
HPC(1.2)_800A	53.97	0.40047	0.99997	55.60
HPC(2.4)_800A	101.14	0.30393	0.99810	100.97

**Table 9** Fitted parameters values in Langmuir adsorption isotherm for methylene blue adsorption onto samples after air oxidation.

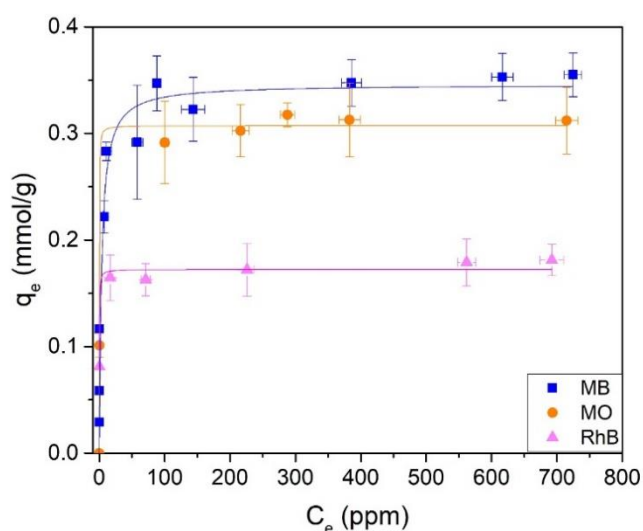


**Figure 14** Adsorption isotherm for methylene blue (MB), methyl orange (MO) and Rhodamine B (RhB) on HPC(2.4)\_800A.

It is well known that surface chemistry and pore structure are the decisive factors for adsorption by carbon adsorbents, the effect of both on the adsorption mechanism and performance has to be therefore considered. According to FTIR, XPS and  $pH_{PZC}$  results discussed above, all the adsorbents should have the same surface chemical properties. For this reason, since all the adsorbents tested in the adsorption studies must be dominated by the  $sp^2$  character rather than the oxygen functionality, the similar interactions between the dye molecules and the adsorbent surface is expected for all adsorbents. This behavior is consistent with previous reports on the  $\pi$ - $\pi$  interactions, in which the  $C=C$   $sp^2$  character is responsible to interact with  $C=C$  bonds of the pi-containing dye molecules. Figure 14 clearly shows the similar molar-adsorption capacities between positively-charged MB (0.35 mmol/g) and negatively-charged MO (0.31 mmol/g) molecules, although the two dyes possess opposite charges. This confirms the independence on electrostatic charge interactions.

Therefore, the different adsorption performances are likely governed by the pore structures of the adsorbents. Intuitively, one may expect larger adsorption capacity by the adsorbents with higher  $S_{BET}$  surface area. Nevertheless, this is not true



in our studies. Although the microporous BG-PGF-800 and BG-PGF-800A show  $S_{\text{BET}}$  exceeding  $600 \text{ m}^2/\text{g}$ , their  $q_{\text{m}}$  values for MB adsorption are only  $4 \text{ mg/g}$ , much lower than that by HPC(2.4)-800A with similar  $S_{\text{BET}}$ . The poor correlations between the  $S_{\text{BET}}$  (surface area), as well as the micropore area and MB adsorption capacity is clearly indicated in Figure 15A and Figure 15B. Since the MB molecule is considered a large molecule with the largest dimension of  $1.70 \text{ nm}$  (Table. 1), the MB molecules cannot access into the abundant microposity with the pore size  $\leq 8 \text{ nm}$  in the non-templated samples; therefore, the pore restriction also occurs. This results in the very low adsorption kinetics and capacity for all these materials. In contrast, both adsorption rate and capacity are much improved by the templated monoliths, which reveal a large contribution of mesoporosity with the size of  $\sim 6 \text{ nm}$ . Interestingly, the linear relationships between MB adsorption capacity and mesopore area and mesopore volume are evidently observed in Figure 15C and Figure 15D, addressing the importance of mesoporosity. The adsorption mechanism related to effect of pore texture is proposed in Figure 16.

Macropores of the raw sugarcane bagasse allowed easy penetration of the template F127 and the carbon precursor into the scaffold; therefore, the high mesopore fraction can eventually be attained. Moreover, the sugarcane bagasse has proved to be a good candidate as a scaffold for the preparation of hierarchical porous carbon. The mesopores with a diameter of  $\sim 6 \text{ nm}$  prepared in our study can be considered as “effective” pores for adsorption of other large dye molecules. MO and RhB were chosen to prove this concept. The adsorption of MO, RhB by HPC(2.4)\_800 reveal  $q_{\text{m}}$  values of  $0.31$  and  $0.18 \text{ mmol/g}$ , respectively. The MO adsorption capacity is similar to that for MB because of their similar molecular dimension, regardless of the electrostatic charge. The  $q_{\text{m}}$  of RhB is lower than those for MB and MO in mol probably because the molecular size of RhB is almost 2 times bigger than those of MB and MO, resulting in small amount of RhB molecules inserting into the effective mesopores. Similarly, the adsorption towards MO and RhB was unsuccessful using the microporous carbons (BG-PGF-800A) with very negligible  $q_{\text{m}}$  of about  $4 \text{ mg/g}$ .

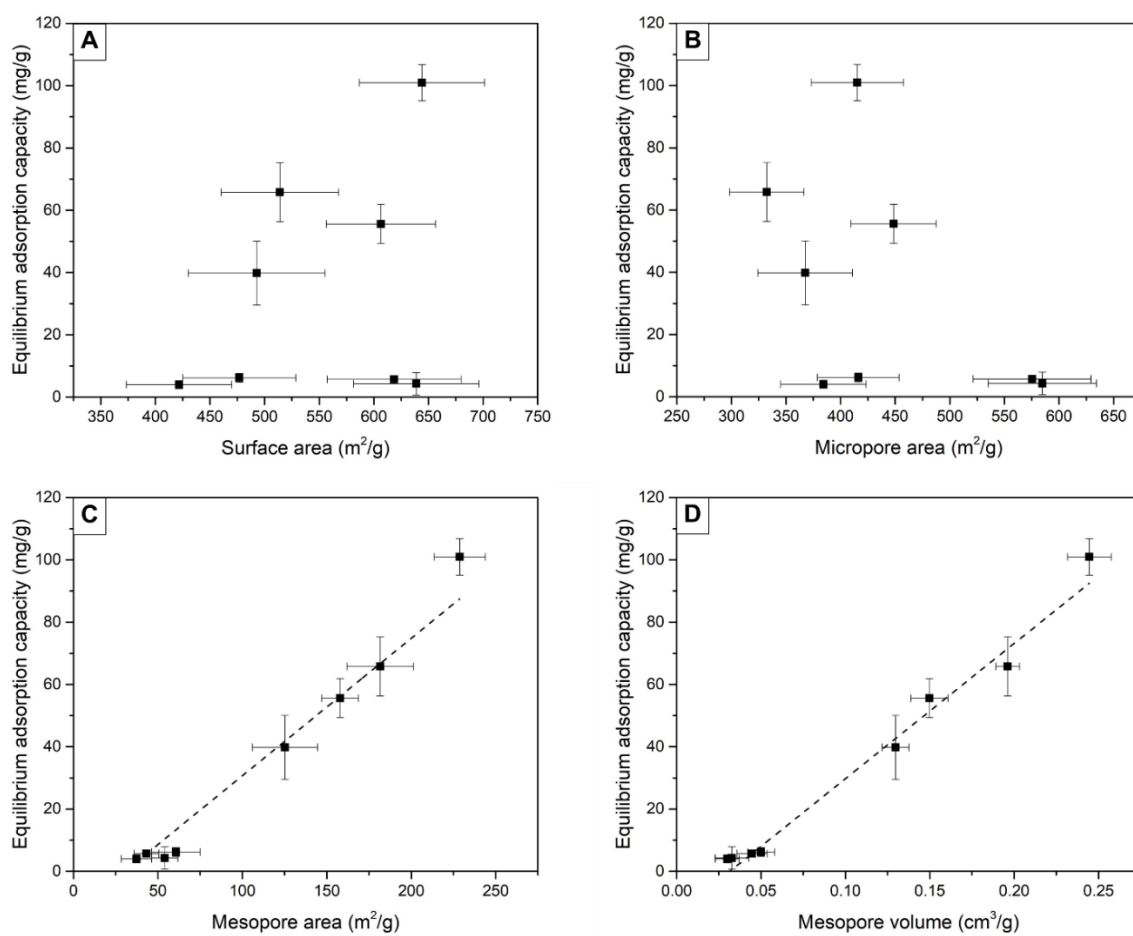


**Figure 15** Correlation of adsorption affinity of different (A) surface area (B) micropore area (C) mesopore area and (D) mesopore volume.

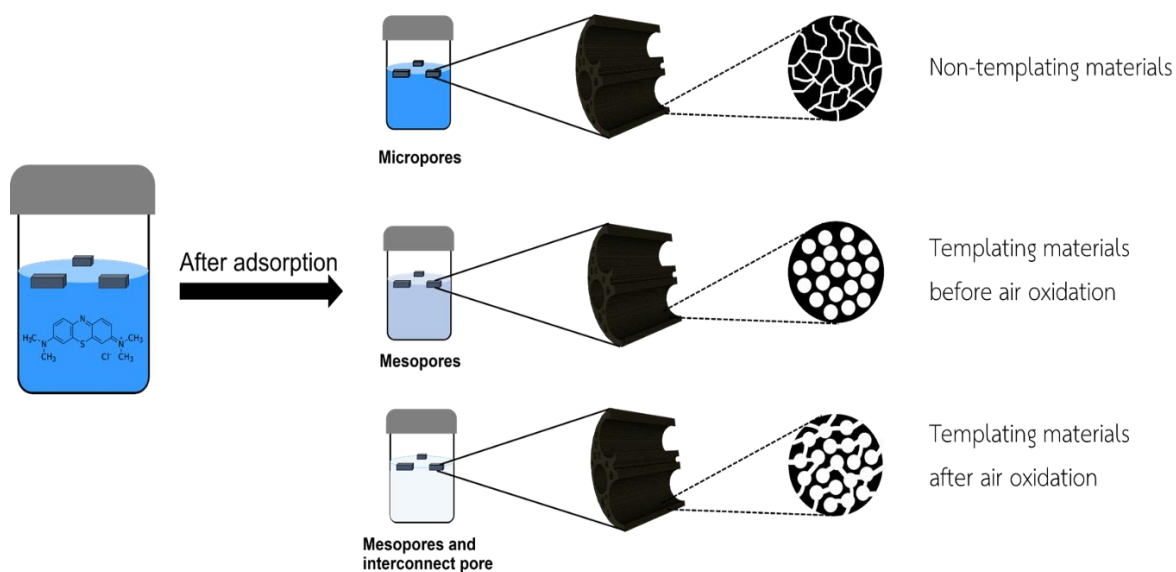


**Figure 16** Schematic Illustration of the effect of pore morphology on the adsorption performance of MB.

To evaluate adsorption capability towards dyes for HPC(2.4)\_800A, comparison of  $q_m$  to those by selected monolithic adsorbents is performed (Table. 9). It is obvious that HPC(2.4)\_800A exhibits the rather high adsorption capacity comparable to other monolithic adsorbents and also even surpass many adsorbents. Despite their slightly higher adsorption capabilities (Table 10) under similar conditions, preparation methods of the monolith adsorbents must be considered. Most monolithic adsorbents require multi-step preparation, large amount of toxic chemicals, for example formaldehyde and strong acid (HCl), high costs of production, therefore making the scalability difficult. Moreover, many works mostly used macroporous polymers as scaffolds. On the contrary, the preparation of the hierarchically porous carbon monoliths reported here employ natural waste, sugarcane bagasse, as a scaffold. More importantly, it requires much milder conditions, evident by the use of phoroglucinol and glyoxylic acid instead of more toxic phenol-formaldehyde. In terms of lower consumption of toxic chemicals usually employed in other preparation, our facile process reported in this work not only reduces time and costs of preparation, but also is considered a greener, more environmentally friendly and efficient for the preparation of hierarchically porous carbon monoliths.

Materials/Adsorbent	Precursor	Binder	Scaffold	Method	S <sub>BET</sub> (m <sup>2</sup> /g)	Pore size (nm)	Dyes	Equilibrium time (h)	k <sub>2</sub> (g mg <sup>-1</sup> min <sup>-1</sup> )	q <sub>e</sub> (mg/g)	Ref
Biomass FA-geopolymer	biomass fly ash waste	metakaolin	-	Geopolymerization	-	-	MB	30	-	15.4	(Novais, Ascensão et al. 2018)
MCCM (F127)	Furfuryl alcohol (FA)	pyrrole	Cordierite monoliths	Dip-coating method	849	21	MB	11 at 50 ppm	2.7 × 10 <sup>-4</sup>	381.5	(Malekbala, Khan et al. 2015)
Acid modified carbon coated monolith (ACCM)	Furfuryl alcohol	pyrrol	Cordierite monoliths	Dip-coating method	237	-	MO	72 at 50 ppm	2.76×10 <sup>-4</sup>	147.06	(Cheah, Hosseini et al. 2013)
Carbon coated monolith (CCM)	Furfuryl alcohol	pyrrol	Cordierite monoliths	Dip-coating method	46.65	mesopore 65% micropore 35%	MO	83.3 at 50 ppm	3.22×10 <sup>-4</sup>	88.5	(Hosseini, Khan et al. 2011)
Mesoporous carbon-based honeycomb monolith	Furfuryl alcohol	pyrrole	Cordierite monoliths	Dip-coating method	352	mesopore 82%	MB	30 at 50 ppm	10×10 <sup>-4</sup>	120.6	(Hosseini, S.Y. Choong et al. 2012)
ZnO@SiO <sub>2</sub> monolith	Zinc nitrate hexahydrate	-	SiO <sub>2</sub> monolith	nanocasting	125	6.5	RhB	1 at 10 ppm	1.1×10 <sup>-4</sup>	500	(Sharma, Hazra et al. 2017)
CA/AC composite monolith	cellulose acetate	-	-	sol-gel method	348	3	MB	50 at 50 ppm	165×10 <sup>-4</sup>	158	(Bai, Xiong et al. 2017)
							RhB	50 at 50 ppm	464×10 <sup>-4</sup>	33.4	
3-D nanofiber aerogels	pullulan/PVA/PAA	-	-	electrospinning	-	-	MB	3 at 200 ppm	4.37×10 <sup>-4</sup>	383.43	(Mousavi, Deuber et al. 2018)
rGO–MMT aerogel	graphene oxide/ montmorillonite	-	-	sol-gel method	43.17	123.28	MB	4 at 40 ppm	2.74	167.79	(Zhang, Yan et al. 2018)
GP aerogel	GO/Poly(ethyleneimine)	-	-	sol-gel method	526.4	3-4	MB	80	0.15×10 <sup>-4</sup>	249.6	(Zhao, Zhu et al. 2018)
							MO	100	0.097×10 <sup>-4</sup>	331	
							MB	24 at 40 ppm	7.5 × 10 <sup>-3</sup>	100.9	
HPC(2.4)_800A	Phloroglucinol / glyoxylic acid	-	bagasse	Wet impregnation	644	5.4	MO	48 at 40 ppm	2.9 × 10 <sup>-3</sup>	103.91	This work

**Table 10** Literature review on monolith adsorbents for dye removal and results.

### 3.3.3 Adsorbent regeneration of hierarchically porous carbon monoliths

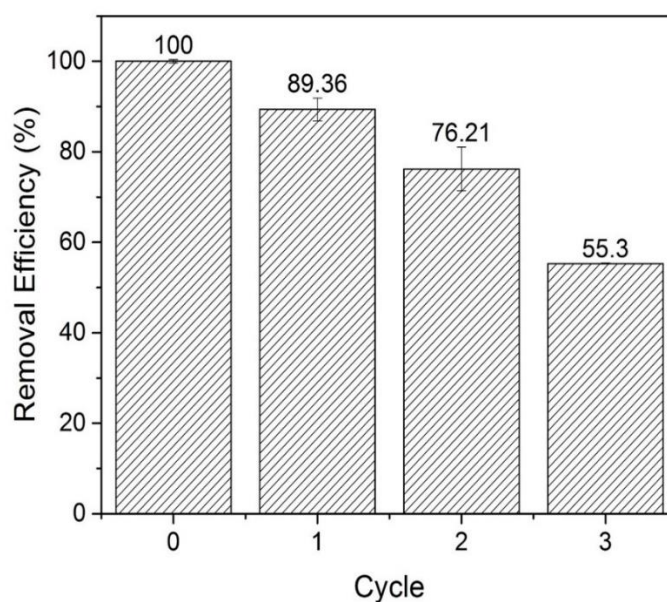


**Figure 17** The reusability of HPC(2.4)\_800A.

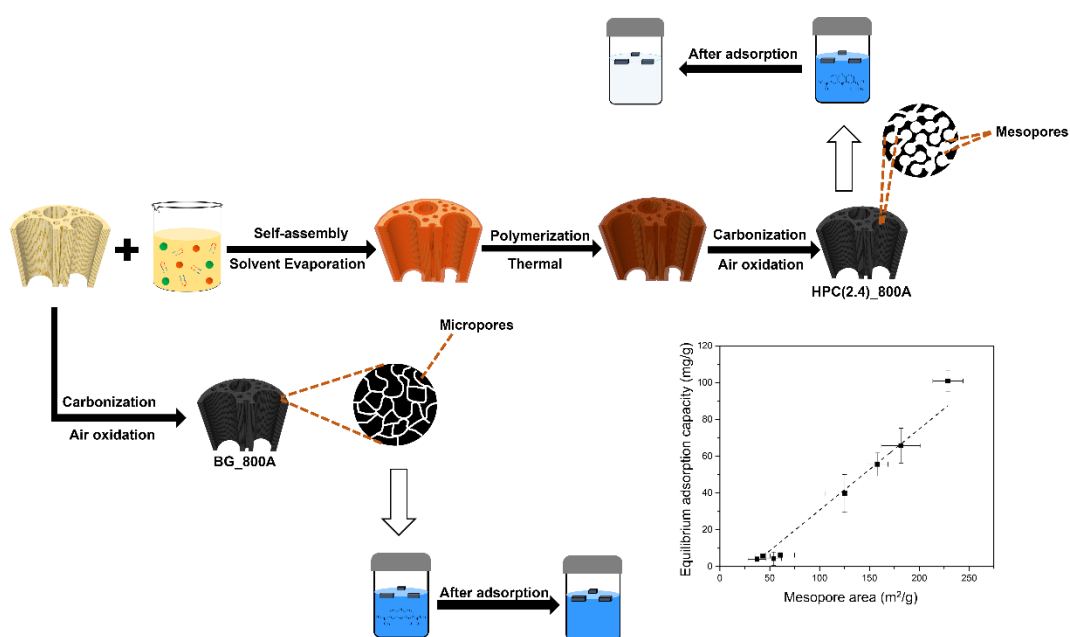
To provide the information on cost effectiveness in industrial scale applications, reusability of the adsorbents was also investigated. Various solvents, including HCl, H<sub>2</sub>SO<sub>4</sub>, NaOH, ethanol and methanol were used in an attempt to desorb the MB from the MB-loaded HPC(2.4)\_800A. Nevertheless, the amount of MB desorbed was rather low with a maximum release only about 5% for all the solvents. This however indicates the strong attachment of MB onto the carbon surface through pi-pi interactions in the mesopore confinement, making the desorption using solubility in solvents difficult to obtain. However, the regeneration of adsorbent was successfully achieved by the heat treatment under N<sub>2</sub> atmosphere at 500°C only for 1h with ramp of 5°C/min in order to remove dye molecules adsorbed on the surface of adsorbent.

The adsorption-desorption cycles by this method were performed to study the reusability of HPC(2.4)\_800A, and the removal efficiency in each cycle is shown in Figure 17. After the first cycle, the adsorption performance dropped to 89.36 %, and further decreased to 55.30 % in the third cycle. Even after the third cycle, the monolithic feature of the sample can still be maintained, proving its high thermal and mechanical stability. In other word, the result suggests that the carbon monoliths can

be regenerated with good adsorption properties and can easily be collected after adsorption process even using for 3 cycles. This will reduce operating costs in the industries. After the end of 5 cycles, no further trials were carried out due to the severe shrinkage of the sample, although the monolith shape was still maintained

## CHAPTER 4

## CONCLUSION



Hierarchically porous carbon materials (HPCs) with macro- and mesoporosity were successfully prepared by surface self-assembly coating of environmentally friendly phloroglucinol/glyoxylic acid precursors, F127 as the template and sugarcane bagasse as scaffold, followed by pyrolysis under inert atmosphere and facile heat treatment. Various techniques was used for investigation of chemical and physical properties. The resulting material showed mesopore structure, high mechanical and chemical stabilities and good dye adsorption performance.

## BIBLIOGRAPHY

- Bai, Q., Q. Xiong, C. Li, Y. Shen and H. Uyama (2017). "Hierarchical porous cellulose/activated carbon composite monolith for efficient adsorption of dyes." Cellulose **24**(10): 4275-4289.
- Bastami, T. R. and M. H. Entezari (2012). "Activated carbon from carrot dross combined with magnetite nanoparticles for the efficient removal of p-nitrophenol from aqueous solution." Chemical Engineering Journal **210**: 510-519.
- Bhatnagar, A. and M. Sillanpää (2010). "Utilization of agro-industrial and municipal waste materials as potential adsorbents for water treatment—A review." Chemical Engineering Journal **157**(2-3): 277-296.
- Cheah, W., S. Hosseini, M. A. Khan, T. G. Chuah and T. S. Y. Choong (2013). "Acid modified carbon coated monolith for methyl orange adsorption." Chemical Engineering Journal **215-216**: 747-754.
- Chen, A., Y. Li, Y. Yu, Y. Li, L. Zhang, H. Lv and L. Liu (2015). "Mesoporous carbonaceous materials prepared from used cigarette filters for efficient phenol adsorption and CO<sub>2</sub> capture." RSC Advances **5**(130): 107299-107306.
- Chen, B., Q. Ma, C. Tan, T.-T. Lim, L. Huang and H. Zhang (2015). "Carbon: Carbon-Based Sorbents with Three-Dimensional Architectures for Water Remediation (Small 27/2015)." Small **11**(27): 3388-3388.
- Chuenchom, L., R. Kraehnert and B. M. Smarsly (2012). "Recent progress in soft-templating of porous carbon materials." Soft Matter **8**(42): 10801-10812.
- Deng, W. and B. H. Shanks (2005). "Synthesis of Hierarchically Structured Aluminas under Controlled Hydrodynamic Conditions." Chemistry of Materials **17**(12): 3092-3100.
- Elaigwu, S. E. and G. M. Greenway (2014). "Biomass derived mesoporous carbon monoliths via an evaporation-induced self-assembly." Materials Letters **115**: 117-120.
- Gupta, V. K. and Suhas (2009). "Application of low-cost adsorbents for dye removal – A review." Journal of Environmental Management **90**(8): 2313-2342.
- Hosseini, S., M. A. Khan, M. R. Malekbala, W. Cheah and T. S. Y. Choong (2011). "Carbon coated monolith, a mesoporous material for the removal of methyl orange



- from aqueous phase: Adsorption and desorption studies." Chemical Engineering Journal **171**(3): 1124-1131.
- Hosseini, S., T. S.Y. Choong and M. Hamid (2012). Adsorption of a cationic dye from aqueous solution on mesoporous carbon-based honeycomb monolith.
- Huang, C.-H. and R.-A. Doong (2012). "Sugarcane bagasse as the scaffold for mass production of hierarchically porous carbon monoliths by surface self-assembly." Microporous and Mesoporous Materials **147**(1): 47-52.
- Li, Y., X.-Y. Yang, G. Tian, A. Vantomme, J. Yu, G. Van Tendeloo and B.-L. Su (2010). "Chemistry of Trimethyl Aluminum: A Spontaneous Route to Thermally Stable 3D Crystalline Macroporous Alumina Foams with a Hierarchy of Pore Sizes." Chemistry of Materials **22**(10): 3251-3258.
- Machoke, A. G., A. M. Beltrán, A. Inayat, B. Winter, T. Weissenberger, N. Kruse, R. Güttel, E. Spiecker and W. Schwieger (2015). "Micro/Macroporous System: MFI-Type Zeolite Crystals with Embedded Macropores." Advanced Materials **27**(6): 1066-1070.
- Malekbala, M. R., M. A. Khan, S. Hosseini, L. C. Abdullah and T. S. Y. Choong (2015). "Adsorption/desorption of cationic dye on surfactant modified mesoporous carbon coated monolith: Equilibrium, kinetic and thermodynamic studies." Journal of Industrial and Engineering Chemistry **21**: 369-377.
- Malik, P. K. (2004). "Dye removal from wastewater using activated carbon developed from sawdust: adsorption equilibrium and kinetics." Journal of Hazardous Materials **113**(1-3): 81-88.
- Martins, L., M. A. Alves Rosa, S. H. Pulcinelli and C. V. Santilli (2010). "Preparation of hierarchically structured porous aluminas by a dual soft template method." Microporous and Mesoporous Materials **132**(1-2): 268-275.
- Matei Ghimbeu, C., L. Vidal, L. Delmotte, J.-M. Le Meins and C. Vix-Guterl (2014). "Catalyst-free soft-template synthesis of ordered mesoporous carbon tailored using phloroglucinol/glyoxylic acid environmentally friendly precursors." Green Chemistry **16**(6): 3079-3088.

- Mousavi, S., F. Deuber, S. Petrozzi, L. Federer, M. Aliabadi, F. Shahraki and C. Adlhart (2018). "Efficient dye adsorption by highly porous nanofiber aerogels." Colloids and Surfaces A: Physicochemical and Engineering Aspects **547**: 117-125.
- Novais, R. M., G. Ascensão, D. M. Tobaldi, M. P. Seabra and J. A. Labrincha (2018). "Biomass fly ash geopolymer monoliths for effective methylene blue removal from wastewaters." Journal of Cleaner Production **171**: 783-794.
- Sharma, M., S. Hazra and S. Basu (2017). "Kinetic and isotherm studies on adsorption of toxic pollutants using porous ZnO@SiO<sub>2</sub> monolith." Journal of Colloid and Interface Science **504**: 669-679.
- Stafiej, A. and K. Pyrzynska (2007). "Adsorption of heavy metal ions with carbon nanotubes." Separation and Purification Technology **58**(1): 49-52.
- Sun, M., C. Chen, L. Chen and B. Su (2016). "Hierarchically porous materials: Synthesis strategies and emerging applications." Frontiers of Chemical Science and Engineering **10**(3): 301-347.
- Vorosmarty, C. J., P. B. McIntyre, M. O. Gessner, D. Dudgeon, A. Prusevich, P. Green, S. Glidden, S. E. Bunn, C. A. Sullivan, C. R. Liermann and P. M. Davies (2010). "Global threats to human water security and river biodiversity." Nature **467**(7315): 555-561.
- Wan Ngah, W. S. and M. A. K. M. Hanafiah (2008). "Removal of heavy metal ions from wastewater by chemically modified plant wastes as adsorbents: A review." Bioresource Technology **99**(10): 3935-3948.
- Wang, J., C. Xue, Y. Lv, F. Zhang, B. Tu and D. Zhao (2011). "Kilogram-scale synthesis of ordered mesoporous carbons and their electrochemical performance." Carbon **49**(13): 4580-4588.
- Xia, L., X. Li, Y. Wu and M. Rong (2015). "Wood-Derived Carbons with Hierarchical Porous Structures and Monolithic Shapes Prepared by Biological-Template and Self-Assembly Strategies." ACS Sustainable Chemistry & Engineering **3**(8): 1724-1731.
- Yoon, S. B., K. Sohn, J. Y. Kim, C. H. Shin, J. S. Yu and T. Hyeon (2002). "Fabrication of Carbon Capsules with Hollow Macroporous Core/Mesoporous Shell Structures." Advanced Materials **14**(1): 19-21.

- Yuan, Z.-Y., J.-L. Blin and B.-L. Su (2002). "Design of bimodal mesoporous silicas with interconnected pore systems by ammonia post-hydrothermal treatment in the mild-temperature range." Chemical Communications(5): 504-505.
- Zhang, Y., X. Liu and J. Huang (2011). "Hierarchical Mesoporous Silica Nanotubes Derived from Natural Cellulose Substance." ACS Applied Materials & Interfaces **3**(9): 3272-3275.
- Zhang, Y., X. Yan, Y. Yan, D. Chen, L. Huang, J. Zhang, Y. Ke and S. Tan (2018). "The utilization of a three-dimensional reduced graphene oxide and montmorillonite composite aerogel as a multifunctional agent for wastewater treatment." RSC Advances **8**(8): 4239-4248.
- Zhao, Q., X. Zhu and B. Chen (2018). "Stable graphene oxide/poly(ethyleneimine) 3D aerogel with tunable surface charge for high performance selective removal of ionic dyes from water." Chemical Engineering Journal **334**: 1119-1127.
- Zhuang, X., Y. Wan, C. Feng, Y. Shen and D. Zhao (2009). "Highly Efficient Adsorption of Bulky Dye Molecules in Wastewater on Ordered Mesoporous Carbons." Chemistry of Materials **21**(4): 706-716.

## VITAE

Name Miss Ratchadaporn Kueasook

Student ID 5810220062

### Educational Attainment

Degree	Name of Institution	Year of Graduation
Bachelor of Science (Chemistry)	Prince of Songkla University	2014

### Scholarship Awards during Enrolment

- The Faculty of Science Research Fund, Prince of Songkla University, for Research Assistantship (RA, Contract No. 1-2558-02-002), the Department of Chemistry, Graduate School, Prince of Songkla University.
- The Center of Excellence for Innovation in Chemistry (PERCH-CIC), Thailand

### List of Proceeding

- Kueasook, R. and Chuenchom, L. (2018). "Preparation of novel hierarchically magnetic porous carbon monoliths by surface self-assembly coating on sugarcane bagasse scaffold." in Proceeding The 44th Congress on Science and Technology of Thailand (STT 44), Bangkok International Trade & Exhibition Center (BITEC) Thailand: 526-531.